General Research profile

Jip Flapper

9129340

Optimization of intranasal MSC therapy for neonatal hypoxic-ischemic brain injury by osteopontin preconditioning of MSCs

Division of woman and baby

Supervisor:

Sara de Palma

Examinator:

Caroline de Theije

Abstract

Hypoxic ischemic encephalopathy (HIE) is one of the leading causes of infant mortality and development of long-term neurological disabilities. Current treatment options are limited, bringing a need for the development of new innovative treatment methods. Intranasal delivery of mesenchymal stem cells (MSCs) has shown promising results in reducing lesions size and improving motor outcomes in neonatal HIE animal models. However, there is still a room for improvement. MSC preconditioning has been shown as a promising strategy to improve MSC paracrine potency and therapeutic efficacy. This research aims to evaluate the potential of osteopontin (OPN) preconditioning of MSCs prior to intranasal administration as a strategy to increase the MSCs' treatment efficacy. Additionally, this study aims to elucidate the effect of OPN on the secretome and intracellular pathways of MSCs.

This study shows that the secretome of MSCs is changed after preconditioning for 24h with 1000ng/ml OPN. Upregulation of growth supportive and angiogenic genes TGF-b and VEGF was shown using qPCR. Inflammatory genes also seemed to be affected, as indicated by a non-significant upregulation of IL-6 and downregulation of iNOS and COX2 mRNA levels. Finally, there appeared to be an autocrine positive feedback loop activated in MSCs, as OPN mRNA levels were non-significantly upregulated after OPN incubation. Higher sample numbers are needed to confirm these non-significant results. Western blot analysis showed an activation in MSCs of the ERK and AKT pathway after 1 hour of OPN incubation. Additionally, there seemed to be an activation of the NF-κB pathway, most prominently at the early timepoints after incubation. The effect on neurogenesis of OPN preconditioned MSCs (OPN-MSCs) was evaluated in a non-contact MSC/NSC co-culture. OPN-MSCs increased differentiation of neuronal stem cells (NSCs) towards astrocytes and induced NSCs into the formation of more complex neurons. A MSC/microglia non-contact co-culture showed that microglia were activated by LPS and that MSCs were able to reduce activation as measured by TNF-α. OPN-MSC did not further reduce TNF-α secretion compared to naïve MSCs. The overall therapeutic efficacy needs to be elucidated in another *in vivo* mouse study. The changes in the secretome and the increased neurogenic capacity of the OPN-MSCs indicate that there is a potential for therapeutical benefits compared to naïve MSCs for neonatal HIE.

Layman summary

Neonatal hypoxic-ischemic encephalopathy (HIE) is caused by a hypoxic event leading to brain injury around birth, which can lead to abnormal motor functioning and decreased neuronal development. Currently treatment options are extremely limited, thus giving rise to the need for new and improved therapy options.

The brain is able to induce its regenerative capacity after injury by activating neuronal stem cells (NSCs) and promoting regeneration. However, naturally available factors that are upregulated after neonatal brain injury are unable to accomplish full repair. Experimental evidence has shown that stem cell based therapies present a promising treatment strategy for brain regeneration after injury. Mesenchymal stem cells (MSCs) have gained attention as a potential therapy for HIE after intranasal delivery. The proposed mechanisms of action is that the MSCs migrate to the injury site after administration, here they secrete factors which activate NSCs. In turn, these NSCs migrate to the area of injury where they restore the injured tissue. Preconditioning, the incubation of the MSCs with certain factors before administration, has been proposed as a promising strategy to increase the efficacy MSC therapy and their regenerative mechanisms. MSC preconditioning with the protein osteopontin (OPN) was indicated as a promising option. In this research the potential of OPN preconditioning of MSCs prior to intranasal administration was evaluated as a strategy to increase the efficacy of intranasal MSC treatment. Furthermore, the effect of OPN incubation on MSCs was investigated through analysis of secreted factors and activation of intracellular pathways.

It was shown that OPN incubation changes the manner how MSCs secrete certain factors, measured by the level of mRNA with qPCR. Particular genes which support growth and the formation of blood vessels, TGF-b and VEGF, mRNA levels were upregulated. Additionally, genes involved with the immune system and inflammation also seemed to be affected, as indicated by apparent upregulation of IL-6 and downregulation of iNOS and COX2 mRNA levels. Finally, OPN mRNA levels itself in MSCs seemed to be upregulated after OPN incubation. This indicates that MSCs could be stimulated to produce more OPN ,when OPN secreted from the same cells binds to the receptors on their own surface. Several intracellular pathways showed indications of activation in MSCs after incubation with OPN. The ERK and AKT pathway were activated after 1 hour of OPN incubation. Additionally, there seemed to be an activation of the NF-κB pathway, most prominently at the early timepoint after incubation.

To better understand potential therapeutic effects of OPN preconditioned MSCs (OPN-MSCs), functional effects were examined. The ability of the OPN-MSCs to influence the NSC differentiation was analysed in a MSC/NSC co-culture. OPN-MSCs increased differentiation of NSCs towards astrocytes and induced NSCs into the formation of more complex neurons. A co-culture of OPN-MSCs and microglia, the primary brain resident immune cells, was used to examine the functional effect of OPN-MSCs on inflammation. It was shown that MSC were able to reduce activity of activated microglia, however OPN-MSC did not further reduce pro-inflammatory cytokine secretion compared to naïve MSCs. The overall therapeutic efficacy needs to be elucidated in another *in vivo* mouse study. The changes in the secretome and the effect on NSC differentiation of the OPN-MSCs indicate that there is a potential for therapeutical benefits compared to naïve MSCs for neonatal HIE.

Contents

1. Introduction

1.1 Introduction

The dramatic change from a placental dependant foetus to an independent self-breathing infant during birth represent an extraordinary switch in life. While for most child births this switch of life elapses completely normal, complications might occur impacting glucose exchange and oxygen maintenance in the brain. Consequently, neonatal encephalopathy, a neurological dysfunction caused by brain injury around birth, might develop in the infant[1–4]. Encephalopathy is associated with perinatal mortality and development of various neurological and movement disabilities. The most common form of encephalopathy is hypoxic-ischemic encephalopathy (HIE), which is one of the major causes of neonatal death and accounts for one of the highest numbers of disability adjusted life years for a single condition.[1,5–8]. In high income countries HIE occurs in approximately 1-2 per 1000 live births[1,4].

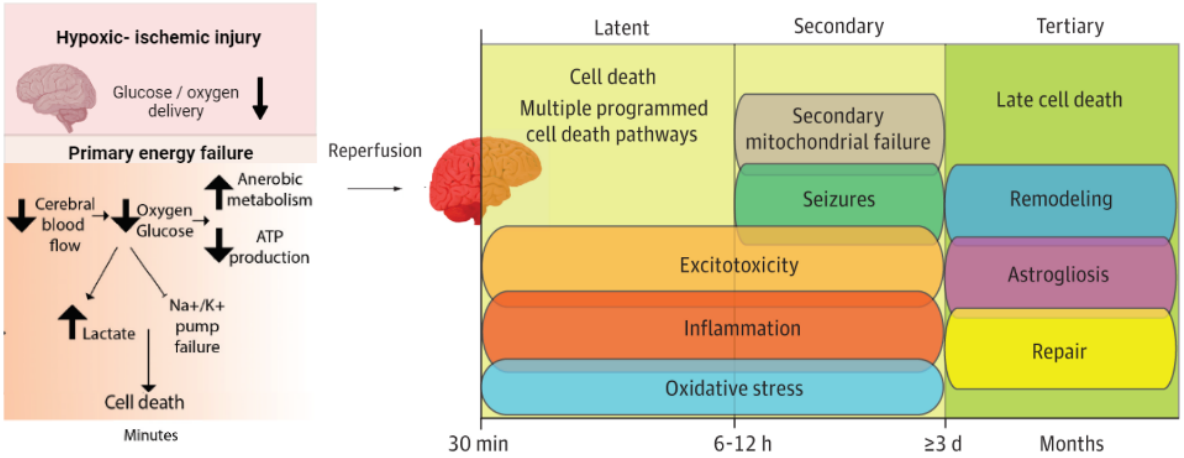

Figure 1 – Schematic overview of HIE pathophysiology. *HIE pathophysiological progression including the acute injury phase with primary energy failure, latent phase characterized by reperfusion, secondary injury phase and tertiary phase of long-term complications. Figure adapted from Douglas-Escobar M, Weiss MD. Hypoxic-Ischemic Encephalopathy A Review for the Clinician. 2015;169(4):397-403. doi:10.1001/JAMAPEDIATRICS.2014.3269 & Worden LT, Massey SL. Therapeutic Hypothermia Effects on Brain Development. Pract Neurol. 2020;(March/April):31-46. https://practicalneurology.com/articles/2020-mar-apr/therapeutic-hypothermia-effects-on-brain-development*[9,10].

HIE pathophysiology progresses over minutes to hours to days and can be described by several phases (Fig 1). A perinatal asphyxia event, such as deficient blood flow, insufficient inspired oxygen or inadequate blood oxygen carrying capacity, is the primary cause of encephalopathy in case of HIE[11]. This primary phase of reduced oxygen and glucose supply to neurons and glia causes a disruption in normal homeostasis. Intracellular energy dependent mechanisms start to fail due to an insufficient supply of high-energy metabolites[12,13]. Na^+ / K^+ pump failure, reduced ATP production, influx of intracellular calcium and neurotransmitters and increased lactic acid lead to ATP depletion, anoxic depolarization, cell swelling, oxidative stress, excitotoxicity and cell death. The next phase, called the latent phase, occurs 1 to 6 hours after injury and is characterized by reperfusion and partial recovery. Re-oxygenation restores the oxidative metabolism and mitochondrial activity[11]. The duration and severity of the asphyxia event is detrimental for the level of recovery of oxidative metabolism[14]. Even though many neurons initially recover from the injury in this phase, there is an ongoing induction of inflammation and intracellular apoptotic cascades. Following the latent phase, a secondary injury occurs 6 hours to 3 days after the initial damage. Delayed energy failure due to recurrent malfunctioning of mitochondrial metabolism, persistent inflammation, cytotoxic edema, oxidative stress and excitotoxicity lead to cell death and delayed deterioration of the brain tissue[11,12].

Despite the fact that the secondary injury phase is resolved approximately 3 days after injury, ongoing effects on the brain persist for days, months or even years[15]. This describes the so called "tertiary phase", which encompasses all the long-term effects, including persistent inflammation and gliosis, impaired oligodendrocyte maturation and myelination and sensitization to injury.

Existing treatment options are mainly limited to supportive care. Therapeutic hypothermia is the only available option to alleviate neurological consequences[16,17]. During hypothermia, the baby's brain is cooled down to a temperature of 33-34°C, thereby slowing cascades that cause widespread damage. However, the treatment has a short therapeutic window, only in the latent phase (6 hours after HIE) does cooling down slow the induction of detrimental cascades. Additionally, the treatment is only partially effective. Thus, there is a dire need for new and more effective treatment options that have a longer therapeutic window.

Animal models of neonatal HIE have shown that the brain is able to activate its endogenous regenerative capacity after injury by activating neuronal stem cells (NSCs) and increasing neurogenesis[18,19]. However, endogenous upregulated factors are unable to induce and maintain long-term neurogenesis, thus fail to accomplish adequate repair. Experimental evidence has shown that stem cell based therapies present a promising treatment strategy for brain regeneration after injury[20]. The intrinsic capacity for self-renewal and the ability to differentiate in various cell types are characteristics which make stem cells suitable for regenerative therapy. Different types of stem cells from different tissue sources exist, each with their own advantageous and disadvantageous properties. Mesenchymal stem cells (MSCs) have gained attention as a potential therapy for HIE due to their potent neuro-regenerative properties, immunosuppressive and anti-inflammatory effects, low immunogenicity, ability to migrate to inflamed sites of injury and relative easy accessible and available sources[20–25]. Furthermore, their low expression of major histocompatibility complex class-II antigens allows for both autologous and allogenic transplantation. Transplantation of MSCs has been shown to enhance the endogenous regenerative capacity of neonatal brains after HIE in several animal models by stimulating NSCs and thereby inducing neurogenesis[24,26–28 29]. Systemic and local delivery routes have been explored for MSC delivery to the sites of injury in the neonatal brain. Even though the systemic delivery route has shown improvements in functional outcomes, the effective cell numbers in targeted organs is lower compared to local delivery due to loss of MSCs in the vasculature [24,28,3031,32]. Furthermore, it is hypothesized that there is further loss of MSCs due to migration to other inflamed organs besides the brain, due to systemic inflammation in infants suffering from HIE[25,33]. Hence, local delivery is thought to be more effective. Local administration of MSCs through intracranial delivery is regularly used in animal models, however direct administration into the brain is a highly invasive procedure and not favourable for translation towards clinical applications [26,34]. Intranasal administration has been emerging as an effective and non-invasive delivery route for MSC transplantation[35]. Various animal models and a first-in-human study showed efficacy and feasibility of intranasal bone marrow derived MSC administration in neonates after HIE[27,35–37]. Lesion sizes in HIE mouse models could be reduced from 30% loss of ipsilateral area to 10-15%, and the MSC induced improvements in lesion size were associated with improvements of sensorimotor and cognitive functioning[27,36]. The hypothesized mechanisms of action is that after transplantation the cells migrate to the site of injury.[26,29]. There, the hypoxic ischemic environment triggers the MSCs to activate their regenerative mechanisms[38]. These mechanisms are not based on MSCs differentiating and integrating into to the damaged neuronal tissue, but rather the induction of a repair promoting milieu to support neurogenesis by release of a pro-regenerative secretome[27]. The paracrine effects of MSCs are thought to drive the stimulation of neurogenesis as well as other effects such as reduced apoptosis, reduced neuroinflammation, increased angiogenesis and diminished scar formation[20,21,23,26,27]. The MSC secretome consists of a wide variety of growth factors

and anti-inflammatory cytokines, such as brain-derived neurotrophic factor (BDNF), vascular endothelial growth factor (VEGF) and nerve growth factor (NGF), which effectuate these processes (Fig 2).

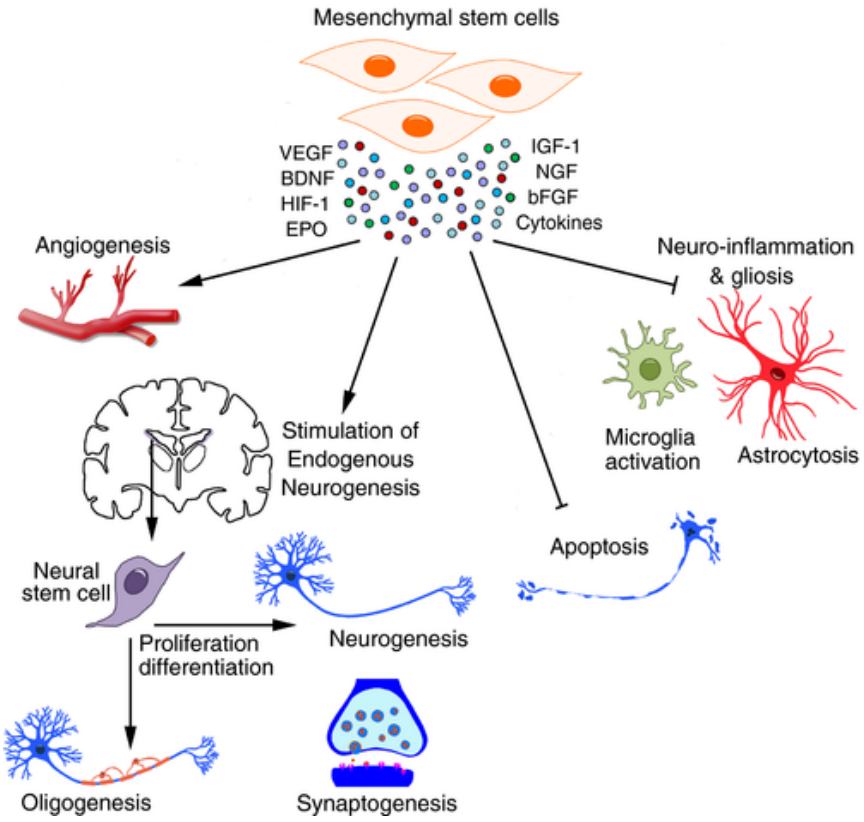

Figure 2 - Various growth factors, such as BDNF, VEGF, NGF, insulin-like growth factor (IGF-1), Fibroblast growth factor 2 (bFGF), Hypoxia inducible factor 1 (HIF-1), Erythropoietin (EPO), and anti-inflammatory cytokines are included in the MSC secretome*. The paracrine signalling induce angiogenesis and neurogenesis, as well as inhibit apoptosis and neuro-inflammation and gliosis. Figure from Wagenaar N, Nijboer CH, van Bel F. Repair of neonatal brain injury: bringing stem cell-based therapy into clinical practice. Dev Med Child Neurol. 2017;59(10):997-1003. doi:10.1111/DMCN.13528/ABSTRACT*[33].

Despite the efficacy MSC therapy has shown over the years in animals models of neonatal HIE, a window for improvement is still left. Various approaches have been investigated to increase the efficacy of MSCs used for therapy and their regenerative mechanisms. The manipulation of MSCs before transplantation, thereby effecting their secretome, has gained attention as a promising option. Recent findings suggest that *in vitro* preconditioning of MSCs can successfully increase paracrine potency and therapeutic potential[39]. A plethora of external cues can be utilized to influence the secretome of MSCs. Not only substances or molecules, such as inflammatory agents, hormones, growth factors, chemical agents or pharmacological agents, can be applied to MSCs, but also variations in external environmental factors, like exposure to hypoxia, can be used for MSC preconditioning[40–47].

Hypoxic preconditioning of MSC has shown to increase the therapeutic efficacy of MSCs in a neonatal HIE animal model (unpublished data). Additionally, the hypoxic preconditioned MSCs showed *in vitro* an enhanced migratory capacity and an increased neurogenic effect. Furthermore, they enhanced secretion of various trophic factors associated with neuronal growth and development. From this study also emerged that osteopontin (OPN) was significantly upregulated in

hypoxic preconditioned MSCs. OPN is a systemically expressed multifunctional protein which is upregulated in various organs in response to inflammation and injury [48–50]. A plethora of cellular signalling pathways, including cytoskeletal organization, membrane ruffling, proliferation and apoptosis, are triggered when OPN is binding to CD44 or its various partial integrin receptors. This involvement in a number of cellular cascades results in the participation of OPN in cell adhesion, chemotaxis, angiogenesis, bone remodelling, wound healing, immunological responses and cell survival.

OPN itself has been shown to enhance the NSC differentiation towards more complex neurons, as well as increase migratory capacity of MSCs (unpublished data)[51]. These findings suggested that OPN can be an important factor in the increased efficacy of hypoxic preconditioned MSCs. Further, different studies have implicated *in vitro* a positive influence of OPN on the neurogenic process of the developing brain through enhanced induction of neuronal differentiation, migration and proliferation of NSCs[52–54]. Moreover, *in vivo* studies have shown exacerbation of HIE in $OPN^{-/-}$ mice and demonstrated that neuroblast migration to the ischemic brain areas depends on OPN [54,55]. The upregulation of OPN in the early stages of spinal cord injury in rats suggests a role in cell proliferation and tissue remodelling [56]. Additional roles of OPN in angiogenesis and various immune or inflammatory functions suggests a diverse impact on various cellular functions[57–59]. Supplementation of OPN to human umbilical vein endothelial cells resulted in improved angiogenic properties[59]. Another study showed that intracerebral haemorrhage induced brain inflammation in hyperglycaemic rats could be attenuated by OPN administration[58].

Taken together this leads to the hypothesis that OPN preconditioning of MSCs prior to intranasal application, will lead to enhanced MSC migration and improved anti-inflammatory capacity, and thereby a better therapeutic efficacy of MSC therapy after neonatal brain injury.

1.2 Research project

The research will consist of two parts, an *in vitro* part and an *in vivo* part. MSCs will be preconditioned with OPN for 24 hours (OPN-MSCs). The effects of OPN preconditioning on MSCs will be assessed in MSC cultures using qPCR and Western Blot to investigate the affected secretome and intracellular pathways. The effect of OPN-MSC on neuro-regeneration and neuroinflammation will be assessed by co-cultures of OPN-MSCs with NSCs and microglia respectively followed by immunocytochemistry and ELISA. *In vivo,* the effect of OPN preconditioning on the therapeutic efficacy of intranasal MSC therapy will be assessed in a mouse model of neonatal HI by immunohistochemistry of brain tissue to measure the lesion size.

2. Materials and method

2.1 *in vitro*

2.1.1 MSC

Bone marrow derived MSCs from GIBCO® Mice (C57BL/6) were purchased (MSCs, #S1502-100, Invitrogen, Thermo Scientific, Waltham Massachusetts, USA) and cultured according to the manufacturer's instructions in normal MSC medium (DMEM:F12, #31331093, GibcoTM, Thermo Fisher Scientific) supplemented by 1% Penicillin-streptomycin (P/S, #15240-62, GibcoTM), 0.05% Gentamicin (#15710064, GibcoTM) and 10% Fetal Calf Serum (FCS, #A4766801, GibcoTM). Passaging was performed with Dulbecco's Phosphate-Buffered Saline (D-PBS, #14190-144, GibcoTM) for rinsing the cells, TrypLE™ Express Dissociation Reagent (TrypLE, #12604-021, Invitrogen) for cell detachment and 10% FCS MSC medium for TrypLE™ neutralization. The cell were passaged once or twice. For preconditioning with OPN (#O2260, Sigma), the MSC's growth medium was removed and replaced with medium containing OPN (1000ng/mL OPN) or control medium (0ng/mL OPN) 24 hours prior to experiments. The control medium contained 100 ug/ml BSA, the same concentration present in the OPN condition. For MSC-NSC co-culture experiments, MSC medium was changed to DMEM:F12 containing 5% platelet lysate (PL, Lonza, Walkersville, Maryland, USA) and 2U/ml Heparin Sodium Injection (#H3149-10KU, Sigma-Aldrich) at the moment of preconditioning.

2.1.2 NSC

Mouse cortical stem cells (NSCs, # SCR029, Merck) were purchased and cultured in a 6-wells plate (#3516, Corning) as neurospheres according to the manufacturer's instructions in proliferation medium (DMEM:F12 (GibcoTM) supplemented by 2% B27 without Vitamin A (#12587001, Thermo Fisher Sc.) and 1% P/S (GibcoTM)). 20ng/mL of Recombinant Human Fibroblast Growth Factor-basic (bFGF, #100-47, Peprotech, Rocky Hill, New Jersey, USA) and Recombinant Human Heparin Binding EGF-like Growth Factor (EGF, #100-18B, Peprotech) were added daily to stimulate proliferation and retain stemness. NSC were passaged once (P1 to P2) before experiments in the following manner: neurorosphere were collected, centrifuged for 5 minutes at 300g, resuspended and disrupted by pipetting. Single cells were counted on NC-200 (ChemoMetec) and reseeded at a density of 2×10^5 cells per well on a 6-wells plate.

2.1.3 Non-contact MSC-NSC co-culture

NSCs cultured as described above, passaged and cultured for another 3 days. Next, NSCs were collected and plated in 24-wells plates coated with 10µg/mL of PLO (Sigma-Aldrich) and 5µg/mL of Laminin (#L2020, Sigma-Aldrich) at a density of 30.000 cells per well in differentiation medium (DMEM:F12 (GibcoTM) supplemented by 2% B27 custom (#0080085SA, Life Techn. (Invitrogen)) and 1% P/S) in the presence of 20ng/mL of bFGF and of EGF to retain stemness. The next day the bFGF and EGF were removed and the differentiation was started. Meanwhile, preconditioned MSCs were harvested and embedded in Truegel (#True1, Sigma) at a density of 8×10^4 cells per transwell insert (Millicell Hanging Cell Culture PET 0.40µm, #MCHT24H48, Millipore) according to the manufacturer's protocol. After 5h, inserts containing OPN- or naïve-MSC were transferred on plated NSC and co-culture was started (figure 3).

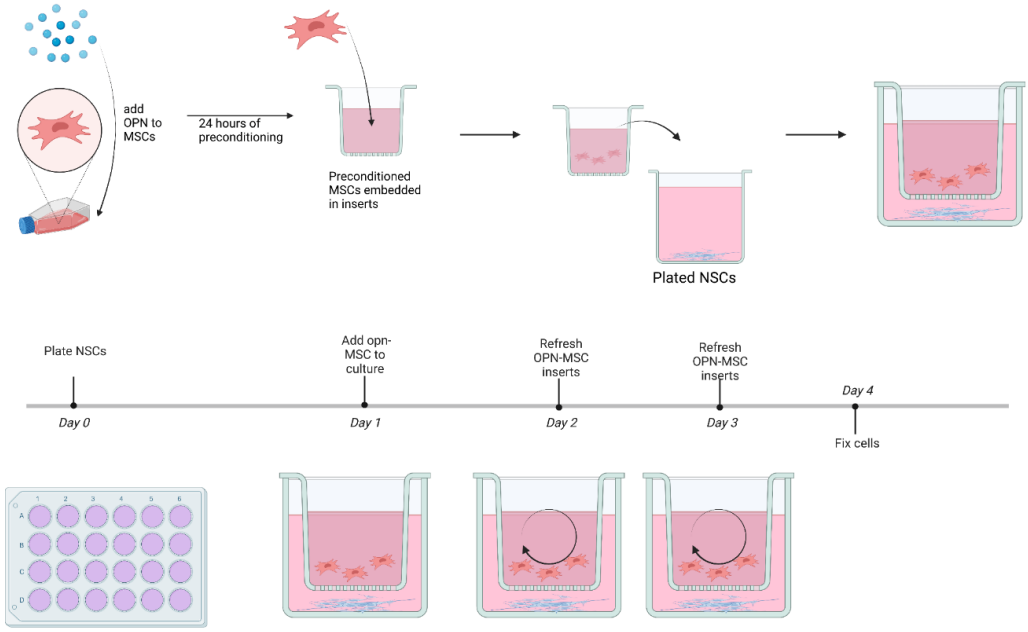

***Figure 3 – Schematic overview of MSC-NSC co-culture**. NSCs are plated in a 24-wells plate, then after 1 day inserts containing naïve MSCs or OPN-MSCs are added and refreshed daily. The OPN-MSC inserts contain MSCs which have been preconditioned with OPN for 24 hours. After three days of co-culture the NSCs were fixated for analysis.*

On day 2 and 3 the inserts were refreshed with similarly as the first day. Inserts without MSCs were used as a negative control condition, these were not refreshed daily. At day 4 the inserts were removed and differentiated NSCs were fixated with 4% PFA (#4078-9020, VWR) in D-PBS.

2.1.4 MSCs co-cultures with microglia and astrocytes

Cortical microglia primary cultures were prepared from C57BL/6 mice from postnatal day 1 or 2. After dissection of the mice pups, meninges were removed and cortices collected. Subsequently, the cortices were minced and incubated with 0.25% trypsin (#T4799, Sigma-Aldrich) in Gey's balanced salt solution (GBSS, #G9779-500mL, Sigma-Aldrich) (containing 1% P/S (GibcoTM), and 30 mM D-(+)-glucose (#G7021, Sigma-Aldrich)) for 10min. After Trypsin removal by centrifugation, cell were resuspended in glia culture medium (DMEM/HamF10 (1:1) (#41965-039 and #31550-023, GibcoTM) supplemented with 10% FCS, 2mM glutamine (#25030024, Invitrogen) and 1% P/S (GibcoTM)) and cultured in poly-L-ornithine-coated flasks (PLO, #P3655, Sigma-Aldrich) (cell suspension of 1 animal/flask). The next day the glia culture medium was refreshed. After 10-12 days in culture, the flasks were shaken at 130-135 rpm for 14-16 hours at 37°C in order to detach microglia. The glia medium containing microglia was collected and centrifuged for 10 minutes at 1200 rpm at RT. Meanwhile, fresh glia medium was added to the flask for a second microglia shake and harvest after another 10 days. Centrifuged microglia were collected, counted, and seeded at a density of 2×10^5 cells per well in a PLO-coated 24-well plate. 24 hours later, preconditioned MSCs were embedded TrueGel in transwell inserts as described in 2.1.3. Embedded MSCs were allow to equilibrate for 3h, after that microglia were stimulated with 50ng/mL lipopolysaccharide (LPS, #L4515, Sigma-Aldrich), immediately followed by the placement of transwell inserts containing MSCs too each well (Fig 4). After 24 hours of co-culture the inserts were removed. Microglia supernantant was collected and stored at -80°C. The plated microglia were fixated with 4% PFA in D-PBS.

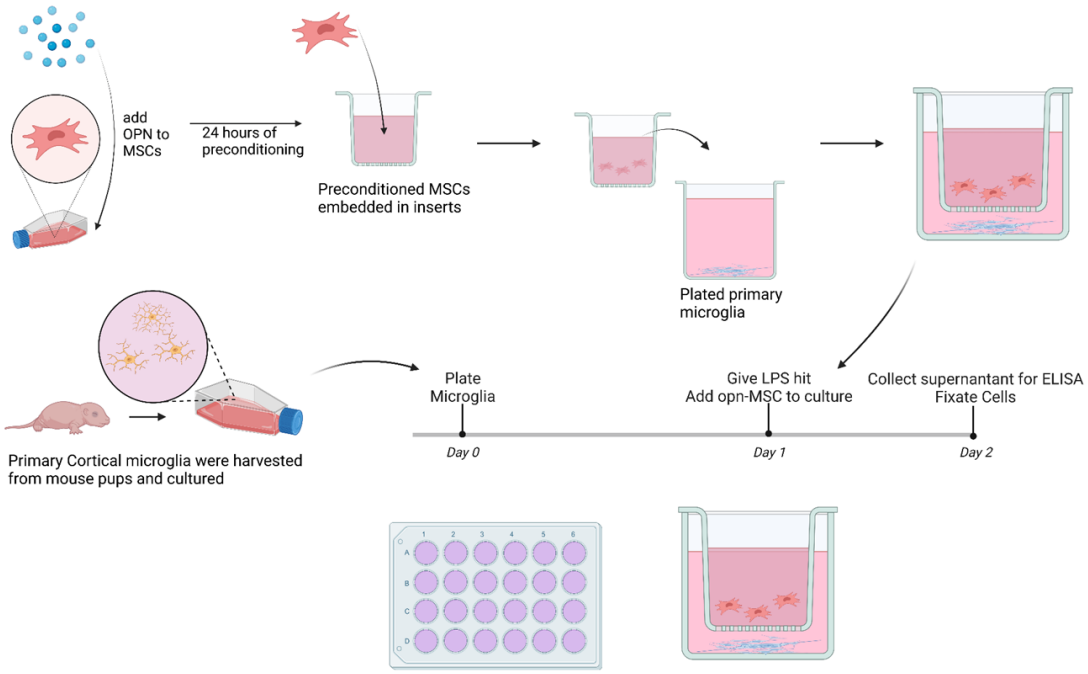

Figure 4 – Schemetic overview of MSC microglia co-culture. *Primary microglia harvested from mouse pups were cultured and plated in a 24-wells plate. After 1 day the microglia were activated with LPS and insets containing naïve MSCs or OPN-MSCs were added. The OPN-MSC inserts contain MSCs which have been preconditioned with OPN for 24 hours. After one day of co-culture supernatant was collected for ELISA and the microglia were fixated for analysis.*

2.1.5 Immunocytochemistry

Non-specific binding on fixated NSC cultures was blocked by incubation in blocking buffer consisting of 2% Bovine Serum Albumin (BSA, #A3059-100G, Sigma-Aldrich) and 0.1% Saponin (#S7900-25G, Sigma-Aldrich) in PBS for at least 25 minutes at RT. Next, the plates were incubated with primary antibodies rabbit anti-βeta-III-tubulin (βIII-tubulin, 1:1000, #Ab18207, Abcam, Cambridge, UK) and mouse anti-GFAP (GFAP, 1:50, BM2287, Origene) for 1 hour at RT, washed with PBS and incubated with conjugated secondary antibodies Alexafluor-594 (1:250, A11012, Invitrogen) and Alexafluor-488 (1:250, A11001, Invitrogen) for 45 minutes at RT. Subsequently the cell nuclei were counterstained with DAPI (1:5000, Merck KGaA) and mounted with FluorSave (VWR). Fluorescent images (n=5 per well) were acquired using an Axio Observer Microscope with Zen software equipped with AxioCam MRm (Carl Zeiss) at 10x/0.3NA magnification. Fiji v.1.53 was used to quantify βIII-tubulin and GFAP area, as well as perform a DAPI count. For each well, values of all acquired pictures were first normalized by DAPI count and then averaged. For each separate co-culture, values were normalized to the naïve MSCs group. To measure neuronal complexity, βIII-tubulin$^+$ positive neurons (minimum n=5 per well) were analysed using the autopath filament tracer algorithm of Imaris v9.2. βIII-tubulin$^+$ neurons were manually traced and neuronal complexity was assessed by total dendrite length, number of branch points, segments, terminal points and Sholl intersections. Neurons were excluded if branches were obscured by nearby cells or background staining and if dendrites were incomplete.

2.1.6 ELISA

TNFα concentrations in microglia supernatant were determined using an ELISA kit for murine TNFα (Ucytech, Utrecht, The Netherlands) according to the protocol form the manufacturer.

2.1.7 qPCR

MSCs were thawed, cultured in T75 flasks at a density of 1×10^6 cells per flaks, passaged once and seeded in a 6-well plate with a density of 2×10^5 cells per well in normal MSC medium. The next day

the MSCs were OPN preconditioned for 24 hours, after which the medium was completely removed and the wells were washed with ice-cold PBS. Cell lysates were collected in RLT buffer (#74104, Qiagen) with b-mercaptoethanol (1:100). From the lysates, RNA was isolated using the RNeasy mini kit (#74104, Qiagen) combined with RNase-Free DNase Set (#79254, Qiagen) for DNase digestion according to the manufacturer's instructions. The RNA quantity of the samples was determined with the Nanodrop 2000 (Thermo Scientific) and quality on OD 260/280 ratio was between 1.97 and 2.3. 0.5µg of RNA was synthesized to cDNA using RT^2 First Strand Kit (#330404, Qiagen) according to the manufacturer's instructions.

The expression of different genes was measured by quantitative reverse transcription (qRT)-PCR (QuantStudio 3, Thermo Scientific) with the use of SYBR green supermix (Biorad, 1708887, Hercules, CA). The primer sequences can be found in Table 1.

GENE	FORWARD PRIMER SEQUENCE	REVERSE PRIMER SEQUENCE
OPN	TGGACTGAGGTCAAAGTCTAGGA	CCGCTCTTCATGTGAGAGGTGA
IL-4	AGATGGATGTGCCAAACGTCCTCA	AATATGCGAAGCACCTTGGAAGCC
IL-6	TCTAATTCATATCTTCAACCAAGAGG	TGGTCCTTAGCCACTCCTTC
IL-10	GCACCCACTTCCCAGTCG	GCATTAAGGAGTCGGTTAGCAG
IL-13	GCCAAGATCTGTGTCTCTCCC	ACTCCATACCATGCTGCCG
IL-1A	CCTTGTGTCCTGTTTAGC	AGGTCTTCTGGTTAGTATCC
INOS	GCACCACCCTCCTCGTTCAG	CCACAACTCGCTCCAAGATTCC
COX2	GGTCTGGTGCCTGGTCTG	CTCTCCTATGAGTATGAGTCTGC
MMP-9	CGCTCATGTACCCGCTGTAT	CCGTGGGAGGTATAGTGGGA
LIF	CTTCTCCCTCTGGTCTCCAA	GGGTCAGGATGTTTCAGCAC
TGF-B	GTGACAGCAAAGATAACAAAC	CTGAAGCAATAGTTGGTATCC
FGF-2	GCGAGAAGAGCGACCCACAC	GAAGCCAGCAGCCGTCCATC
BDNF	CACATTACCTTCCAGCATCTGTTG	ACCATAGTAAGGAAAAGGATGGTCAT
VEGF	GATCCTCTGCCCGCCTTG	CCCGTGGAGTCTGGAAAGC
NGF	ACGGGCAGCATGGTGGAG	TGTAGAACAACATGGACATTACGC

Table 1 – Primer sequences used for qPCR.

2.1.8 Western blot

MSCs were cultured as described above, passaged once and seeded in a 6-well plate at a density of 4×10^5 cells per well in normal MSC medium. The next day the MSCs were preconditioned with OPN for 30 minutes, 1 hour, 2 hours, 3 hours or 24 hours, and after each timepoint the medium was completely removed and the wells were washed with ice-cold PBS. The cells were treated with 500µl lysis buffer containing RIPA buffer (#R0278, Sigma) , Protease inhibitor tablets Complete tablets Mini EDTA free and the phosphate inhibitor NaF (5mM, 1.064.490.250, VWR), and Na3VO4 (1mM, VWR). Cell scrapers were used for cell detachment, after which cell lysates were collected, sonicated on ice for 5 seconds and centrifuged at 13000 rpm for 15 minutes at 4^oC. Supernatant was collected and stored (as whole fraction) in -20^oC until use. Protein levels per sample were quantified using the Bradford protein assay, using Protein assay dye reagent concentrate (500-0006, Biorad) according to the manufacturer's protocol. SKanIt (Thermo Fisher Scientific) software was used to measure

absorbance at 595nm at 20^{o}C including a 0.05 second shake. A linear regression line was used with a regression coefficient (R^2) above 0.98.

4-20% CriterionTM TGXTM precast gels (12+2 well, 45µL, 5671093, Bio-Rad)(18 well, 30µL, 5671094, Bio-Rad) were prepared with running buffer containing 1.44% glycine (4808831, MP biomedicals, California, USA), 0.3% Tris (10708976001, Roche) and 1% SDS (161-0418, Biorad) in demiwater, after which 15 µg of protein was loaded onto each slot. Protein separation ran at 180 V and 400 mA for 1 hour. Separated proteins were transferred onto Nitrocellulose membranes, 0.2µm (#1620112, Bio-rad) at 100 V for 1 hour while submerged in transfer buffer containing 1.44% glycine and 0.3% Tris in demiwater. Then the membranes were washed in washing buffer and stained with Ponceau red, containing 1% Ponceau (P3504-100G, Sigma-Aldrich) and 1% acetic acid (510.000.632.500, Boom), for confirmation of protein separation. After confirmation, the membranes were washed again and incubated with blocking buffer (5% BSA in washing buffer) for 1 hour. Subsequently the membranes were incubated overnight at 4^{o}C with primary antibodies as indicated in Table 2. The next day the membrane was washed with washing buffer and incubated for 1 hour at RT with secondary antibodies as indicated in Table 2 . β-actin incubation and imaging was not directly possible due to overlapping molecular weights, thus gels were stripped of HRP after imaging. The gels were incubated in Sodium-azide (1:1000, #S2002-100G, Sigma) for 20 minutes, washed and stripping effectiveness was confirmed. Then incubation steps of primary and secondary antibodies was repeated for β-actin as described above. Imaging was performed with an ECL kit (RPN2106, Fisher Scientific) according to manufacturer's instructions, and ProXima 2750 imaging system. Values of each sample were normalized against β-actin values.

PROTEIN	PRIMARY ANTIBODY	SECONDARY ANTIBODY
P-AKT (60-62 KDA)	P-Akt (S473) (D9E) XP (R) Rabbit MAb (1:1000, 4060S, Cell signaling technology)	Anti-Rabbit IgG HRP - linked AB (1:2000, 7074, Abcam)
AKT (57KDA)	Akt (pan) (C67E7) Rabbit mAb (1:2000, 4691S, Cell signaling technology)	
P-ERK1/2 (43 KDA)	P-p44/42 MAPK (T202/ Y204) XP(R) Rabbit mAb (1:1000, 4370S, Cell signaling technology)	
ERK1/2 (43 KDA)	p44/42 MAPK (Erk1/2) (137F5) Rabbit mAb (1:2000, 4695S, Cell signaling technology)	
IKB-A (37 KDA)	IκB-α (C-21) SC-371 Rabbit polyclonal (1:1000, L1409, Santa Cruz)	
B-ACTIN (40-50 KDA)	Anti-β-Actin antibody mouse Monoclonal (1:5000, A5316, Sigma)	IgG, Horseradish Peroxidase linked whole antibody (1:5000, A931V, GE Healthcare

Table 2 – Antibodies used for western blot.

2.2 *in vivo*

2.2.1 Animals

The animal experiments were performed in accordance with Dutch and European international guidelines (Directive 86/609, ETS 123, Annex II) and approved by the Experimental Animal Committee Utrecht (University Utrecht, Utrecht, Netherlands) and the Central Authority for

Scientific Procedures on Animals (The Hague, The Netherlands). All efforts were made to minimize suffering.

C57Bl/6 mice (OlaHsa, ENVIGO, Horst, The Netherlands) were kept in standard housing conditions with woodchip bedding, cardboard shelters and tissues provided, on a 12hr day/night cycle (lights on at 7:00), in a temperature-controlled room at 20-24°C and 45-65% humidity with ad libitum food and water access. Mice were bred in-house by placing wild type males and females together in a ratio of 1:1 or 1:2 for two weeks. Afterwards, dams were housed solitarily to give birth. Breeding resulted in 21 litters. Hypoxic-ischemic (HI)-injury was induced in 9-days-old pups by unilateral carotid artery ligation under isoflurane anesthesia ((5–10 min; 5% induction, 3–4% maintenance with flow O2: air 1:1), followed by recovery with their mother for at least 75min and subsequently systemic hypoxia at 10% O2 for 45min in a temperature-controlled hypoxic incubator. A lesion involving the hippocampus, neocortex and striatum was induced by the procedure. Xylocaine (#N01BB02, AstraZeneca, Cambridge, UK) and Bupivacaine (#N01BB01, Actavis, Allergan Inc, Dublin, Ireland) were applied to the wound for pre- and post-operative analgesia. Control SHAM animals were subjected to anesthesia and surgical incision only. Two days after injury, litters received cage enrichment: a turning wheel on a red plastic shelter. MSCs were administered intranasally at 10 days after induction of HI. 30min before intranasal MSC administration, hyaluronidase (100U, #H4272, Sigma-Aldrich, Merck KGaA, Darmstadt Germany) was administrated intranasally to increase permeability of the connective tissue in the nasal cavity. HI-injured mouse pups were treated intranasally with MSC or OPN-MSCs ($5x10^5$ per animal) in D-PBS, or D-PBS only as vehicle treatment, by administration of 2 droplets of 3µL per nostril. The male and female offspring was randomly assigned to four experimental groups: SHAM operated animals (n=18), HI vehicle-treated animals (n=18), HI MSC-treated animals (n=18) and HI OPN preconditioned (OPN)-MSC-treated animals (n=18).

2.2.2 Immunohistochemistry

Animals were sacrificed at day 28 post HI by overdose of pentobarbital (Alfasan, Woerden, The Netherlands), transcardially perfused with Phosphate Buffered Saline (PBS, #524650-1, VWR, Radnor, Pennsylvania, USA) followed by 4% paraformaldehyde, (PFA, #VWRK4078-9020, VWR) and brains were collected. Brains were post-fixed for 24hr and dehydrated followed by embedment in paraffin. Coronal sections (8 µm) were cut at the CA1 hippocampal level (Bregma -1.85). Afterwards, all sections were deparaffinized and hydrated. To assess lesion size, sections were stained with hematoxylin and eosin (H&E). Images were taken at 2.5x magnification. Area measurements of the ipsilateral and contralateral hemispheres were performed by a blinded observer using Adobe Photoshop CS6 and ipsilateral tissue loss was calculated as [1 - (ipsi / contra) x 100%].

2.3 statistical analysis

Statistics were performed using GraphPad Prism 9.3.0 (Graphpad Software). Outliers were identified using the ROUT method (Q = 1%). qPCR data was statistically analysed by unpaired T test. The MSC/NSC co-culture, ELISA and mouse study data were statistically analysed by one-way ANOVA. Differences of $p < 0.05$ were deemed as statistically significant.

3. Results

3.1 OPN changes the gene expression of MSCs

qPCR was used to characterize the changes in gene expression after OPN preconditioning of MSCs. After 24 hours of OPN preconditioning, RNA of the MSCs was collected and used to determine expression level of several genes. Various inflammatory genes were measured to gain insight in the immunomodulatory potential of OPN-MSCs[59]. mRNA levels of IL-6 seemed to be slightly upregulated, whereas pro-inflammatory associated genes iNOS and COX2 seem to be slightly downregulated (Fig 5c, e, f) in OPN-MSC versus naïve MSC, but no significant differences were observed, potentially due to a low number of samples. Additionally, genes involved in tissue repair and angiogenesis were measured. VEGF and TGF-b mRNA levels were significantly upregulated in OPN-MSC compared to naïve MSC (P=0.0231 and P=0.0144 respectively)(Fig 5a, b). No difference was observed after OPN preconditioning of MSCs in the expression levels of FGF, MMP9, BDNF and NGF (Appendix A). Finally, OPN fold change resulted in modest non-significant upregulation after OPN incubation, indicating a potential autocrine positive feedback loop (Fig 5 d).

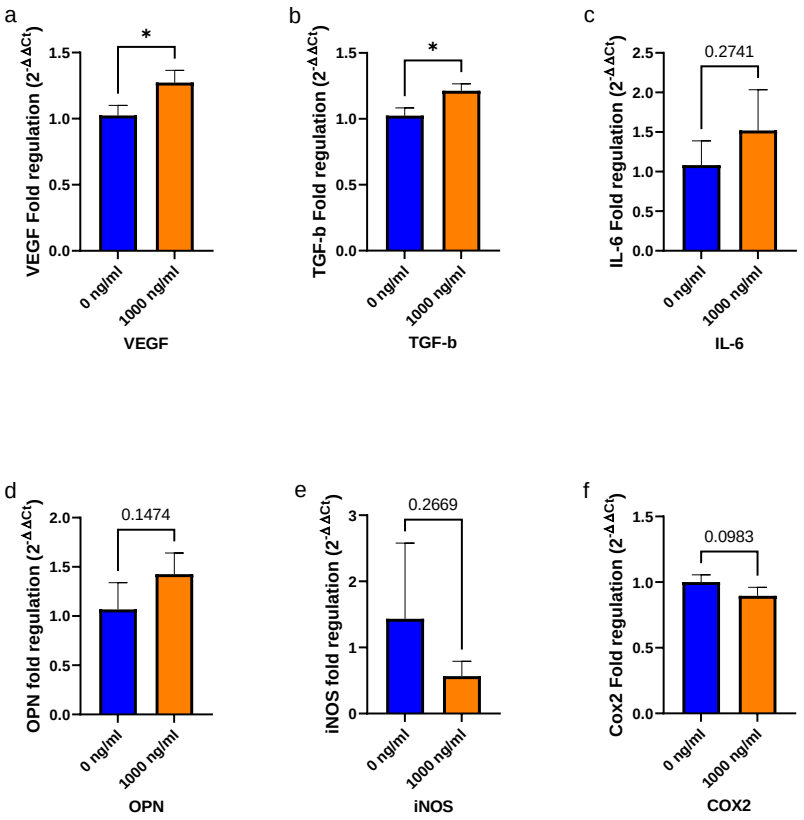

Figure 5 – Gene expression of naïve MSCs compared to MSCs preconditioned with 1000 ng/ml OPN for 24 hours determined by qPCR. (a-g) *Fold regulation of VEGF, TGF-b, IL-6, OPN, iNOS and COX2 mRNA normalized to naïve MSC. Data represents mean ± SEM. Statistical analysis (a-g): unpaired t-test. *(p<0.05). (a-g): n=3*

3.2 OPN activates various intracellular pathways in MSCs

Western blot was performed to determine which cellular pathways were activated by OPN preconditioning of MSCs. Individual expression levels of phosphorylated ERK (pERK), ERK, phosphorylated AKT (pAKT) and AKT were measured at 30 minutes, 1 hour, 2 hours and 24 hours after stimulation with OPN (Fig 6c, d) (Appendix B). The activation state of ERK and AKT were measured as the ratio between their phosphorylated and non-phosphorylated state (Fig 6a, b) [61,62].

Both ERK and AKT follow a similar trend in their activation state. 30 minutes of OPN incubation results in no difference between naïve MSCs and OPN-MSCs in ERK or AKT activation state. Both pathways are highly upregulated at the 1 hour time point of OPN incubation compared to naïve MSCs. At the 2 hour timepoint there seems to be a small decrease in activation compared to naïve MSCs. Finally at the 24 hour timepoint of incubation with OPN there is no difference between naïve MSCs and OPN-MSCs for the ERK or AKT activation state.

In order to look at the inflammatory response that OPN might induce, the NF-kB pathway is of interest [63]. IκB expression was analysed as an indirect measure for NF-kB activation (Fig 6e, f). There seems to be a slight reduction in the presence of IκB protein after MSCs are preconditioned for 30 minutes with OPN compared to naïve MSCs. At the 6 hours timepoint and 24 hours timepoint of incubation with OPN the reduction of IκB protein compared to naïve MSCs is still existing, but in lesser proportions. This could indicate that there is an activation of the NF-kB pathway.

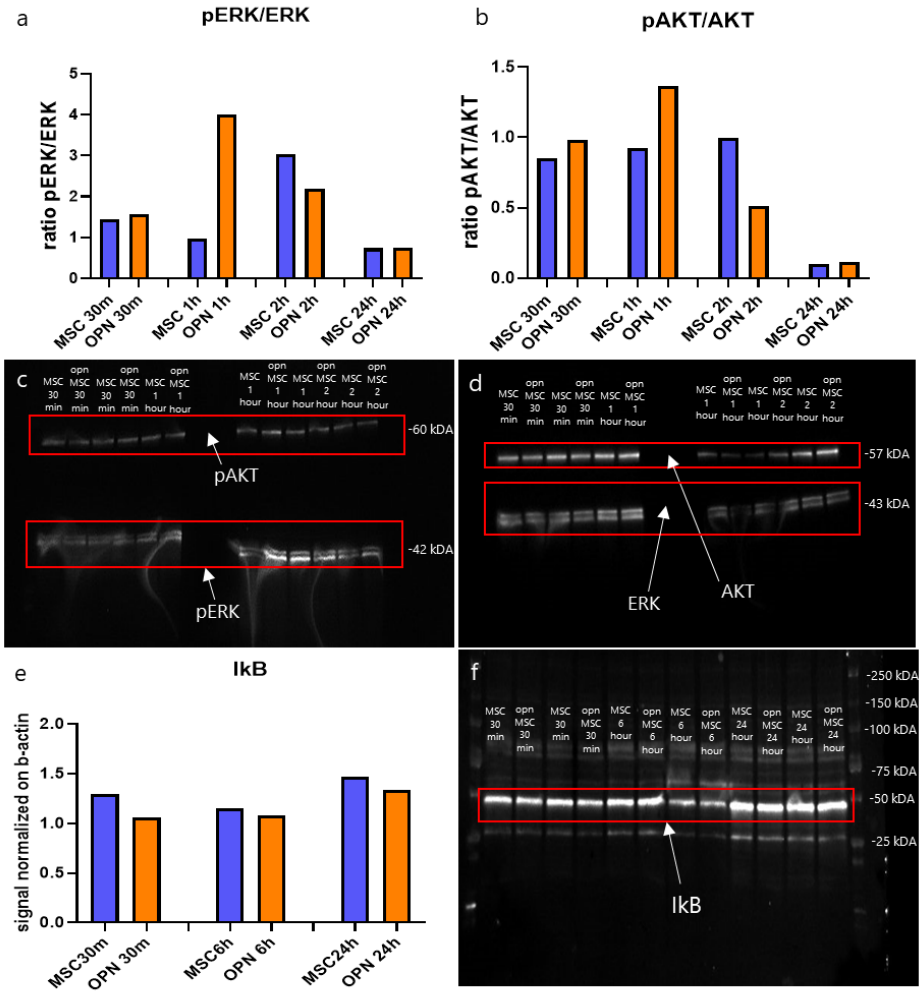

Figure 6 - Western blot analysis of (p)ERK, (p)AKT and IκB expression of MSCs after OPN incubation at different time points. *(**a**) Activation state of ERK in MSCs measured by the ratio of pERK and ERK after 30 minutes, 1 hour, 2hours and 24 hours of incubation with OPN compared to naïve MSCs. (**b**) Activation state of AKT in MSCs measured by the ratio of pAKT and AKT after 30 minutes, 1 hour, 2hours and 24 hours of incubation with OPN compared to naïve MSCs. (**c**) Western blot image of pAKT and pERK expression in MSCs after 30 minutes, 1 hour and 2hours of incubation with OPN compared to naïve MSCs. (**d**) Western blot image of AKT and ERK expression in MSCs after 30 minutes, 1 hour and 2hours of incubation with OPN compared to naïve MSCS. (**e**) Expression of IκB in MSCs after 30 minutes, 6 hours and 24 hours of incubation with OPN compared to naïve MSCs. (**f**) Western blot image of IκB expression in MSCs after 30 minutes, 6 hours and 24 hours of incubation with OPN compared to naïve MSCs. Data represents mean (a-f): MSC n=1, OPN-MSC n=1.*

3.3 Functional effect on neurogenesis

In order to determine the functional effect of OPN-MSCs on neurogenesis, a non-contact MSC/ NSC co-culture was performed. At the start of spontaneous NSC differentiation, NSCs were co-cultured with naïve MSC inserts, OPN-MSC inserts or empty inserts. At 72 hours after the onset of differentiation, the NSCs were fixated and stained for GFAP and βIII tubulin (Fig 7a-d). NSC differentiated in the presence of OPN-MSCs showed a significant increase in the GFAP$^+$ area per DAPI stained nucleus (P=0.007)(Fig 7d) compared to naïve MSC, but no significant increase in the βIII-tubulin$^+$ area per DAPI stained nucleus (Fig 7e, f).

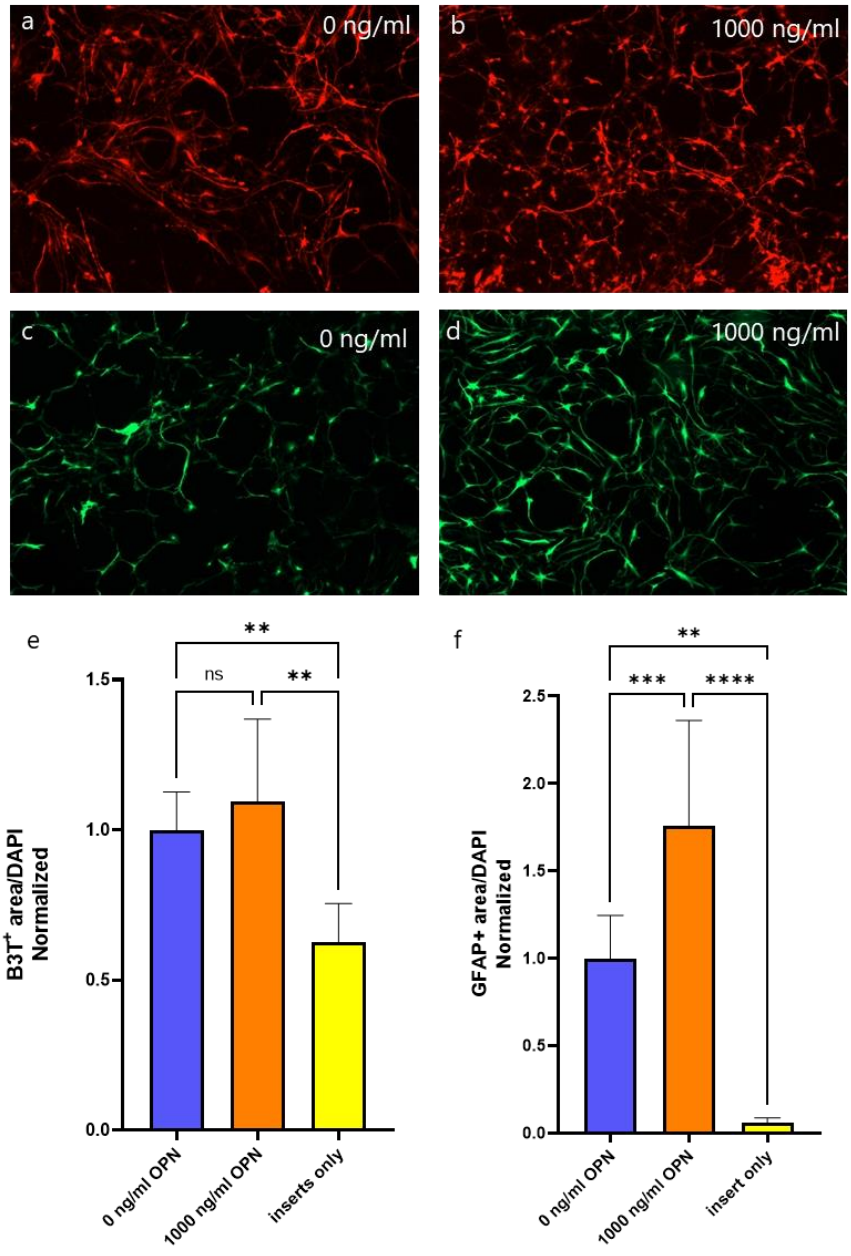

Figure 7 – Area analysis of Non-contact MSC/NSC co-culture. *(**a, b**) 72 hours after the onset of differentiation in the presence of OPN-MSCs (1000ng/ml) and naïve MSCs (0 ng/ml), the NSC were fixated and stained for βIII tubulin (red). (**c, d**) 72 hours after the onset of differentiation in the presence of OPN-MSCs (1000 ng/ml) and naïve MSCs (0 ng/ml), the NSC were fixated and stained for GFAP (green). (**e**) βIII-tubulin+ area per DAPI stained nucleus normalized to naïve MSCs (0 ng/ml). (**f**) GFAP+ area per DAPI stained nucleus normalized to naïve MSCs (0 ng/ml). Data represents mean ± SEM. Statistical analysis (e, f): one-way ANOVA. **(p<0.01), ***(p<0.00.1), ****(p<0.0001). (e, f): 0 ng/ml: n=12, 1000 ng/ml : n=10, inserts only: n=5.*

Additionally, morphological analysis was performed on the formed βIII-tubulin$^+$ neurons. The individual dendrites of βIII-tubulin$^+$ neurons were manually traced and neuronal complexity was assessed (Fig 8a, b). Even though OPN-MSCs did not increase the filament dendrite length (Appendix C), NSCs differentiated in the presence of OPN-MSCs did show a significantly higher number of branch points (P=0.0002), branch segments (P=0.0002) and terminal points (P=0.004) compared to naïve MSCs (Fig 8c-e). Furthermore, there was a significantly higher number of sholl intersections of neurons formed under the influence of OPN-MSCs compared to naïve MSCs (P=0.0064) (Fig 8f, g). These results together suggest an enhanced capability of OPN-MSCs to influence NSC differentiation towards more complex neurons compared to naïve MSCs.

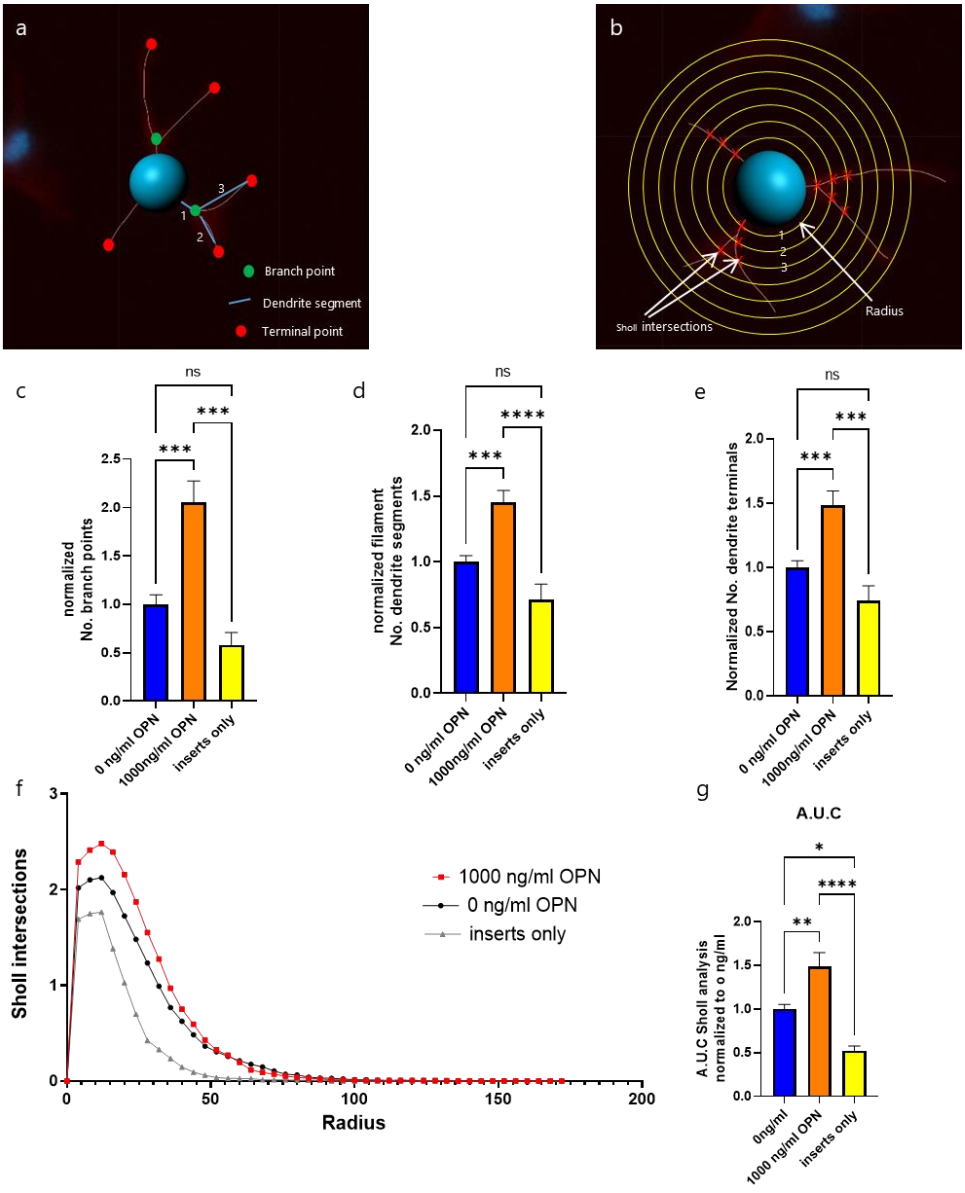

Figure 8 – Morphological analysis of non-contact MSC/NSC co-culture. *(**a**) Overview of the definition of branchpoint, dendrite segment and terminal point during morphological analysis. (**b**) Descriptive overview of the sholl analysis on neurons. (**c**) Number of branch points per neuron normalized to naïve MSCs (0 ng/ml). (**d**) Number of dendrite segments per βIIIT+ neuron normalized to naïve MSCs (0 ng/ml). (**e**) Number of dendrite terminal points per βIIIT+ neuron normalized to naïve MSCs (0 ng/ml). (**f**) Number of intersections of βIIIT+ neurons with circles of increasing radius by Sholl analysis. (**g**) Quantification of Sholl analysis by area under the curve (A.U.C.). Data represents mean ± SEM. Statistical analysis (c-e, g): one-way ANOVA. **(p<0.01), ***(p<0.001), ****(p<0.0001). (c-d, g): 0 ng/ml: n=12, 1000 ng/ml : n=10, inserts only: n=5.*

3.4 Functional effect on inflammation

To determine the functional effect of OPN-MSCs on inflammation, a MSC/microglia co-culture was performed. Primary microglia were stimulated with 50 ng/ml LPS to induce an inflammatory state, directly after which they were co-cultured with naïve MSC inserts, OPN-MSC inserts or empty inserts. 24 hours after initiation of the inflammatory state, the supernatant of microglia was collected and TNF-α secretion was measured by ELISA. Addition of LPS activated the microglia, measured by an upregulation of TNF-α secretion for LPS activated microglia with empty inserts (+LPS inserts only) compared to inactivated microglia with inserts containing OPN-MSCs (-LPS OPN-MSC) or naïve MSCs (-LPS MSC) (Fig 9). MSCs significantly lowered the secretion of TNF-α by microglia (for both P<0,0001) compared to inserts without MSCs (Fig 9). However, no difference was observed between the OPN-MSC's and the naïve MSC's ability to lower excretion of TNF-α from LPS stimulated microglia.

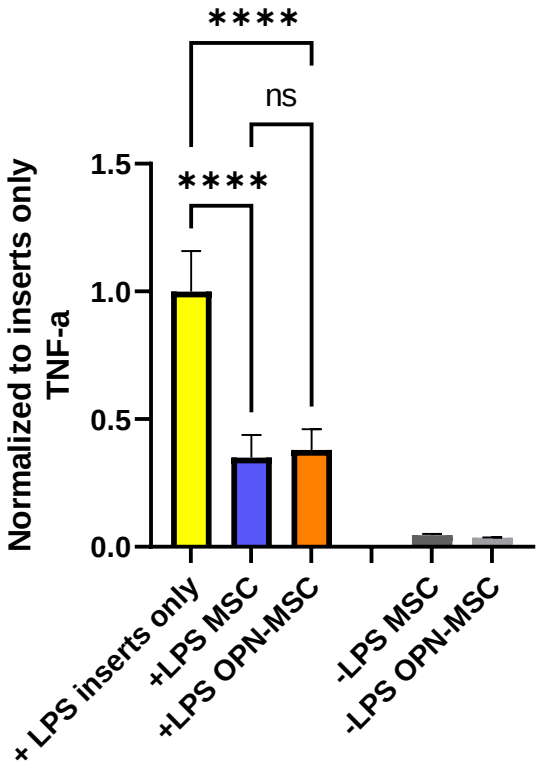

***Figure 9 – ELISA performed on the MSC/microglia co-culture**. ELISA performed on microglia supernatant measuring TNF-α secretion normalized to +LPS inserts only. Data represents mean ± SEM. Statistical analysis (f): one-way ANOVA. ***(p<0.001). (f): -LPS MSC: n=2, -LPS OPN-MSC: n=2, +LPS inserts only: n=18, +LPS MSC: n=18, +LPS OPN-MSC: n=14.*

3.5 Treatment efficacy in a neonatal HIE mouse model

The treatment efficacy of OPN-MSCs compared to naïve MSCs was evaluated in a neonatal HIE mouse model. OPN-MSCS or naïve MSCs were intranasally administered to C57BI/6 mice at D10 after induction of neonatal HIE (Fig 10a). The lesion size was assessed 28 days after induction of neonatal HIE by H&E staining of the brain sections(fig 10b). Animals with HI induced injury showed volume loss in the ipsilateral hemisphere compared to SHAM surgery treated animals (P<0.0001)(Fig 10c). However, both naïve MSCs and OPN-MSCs did not reduce the volume loss after HIE compared to vehicle treatment.

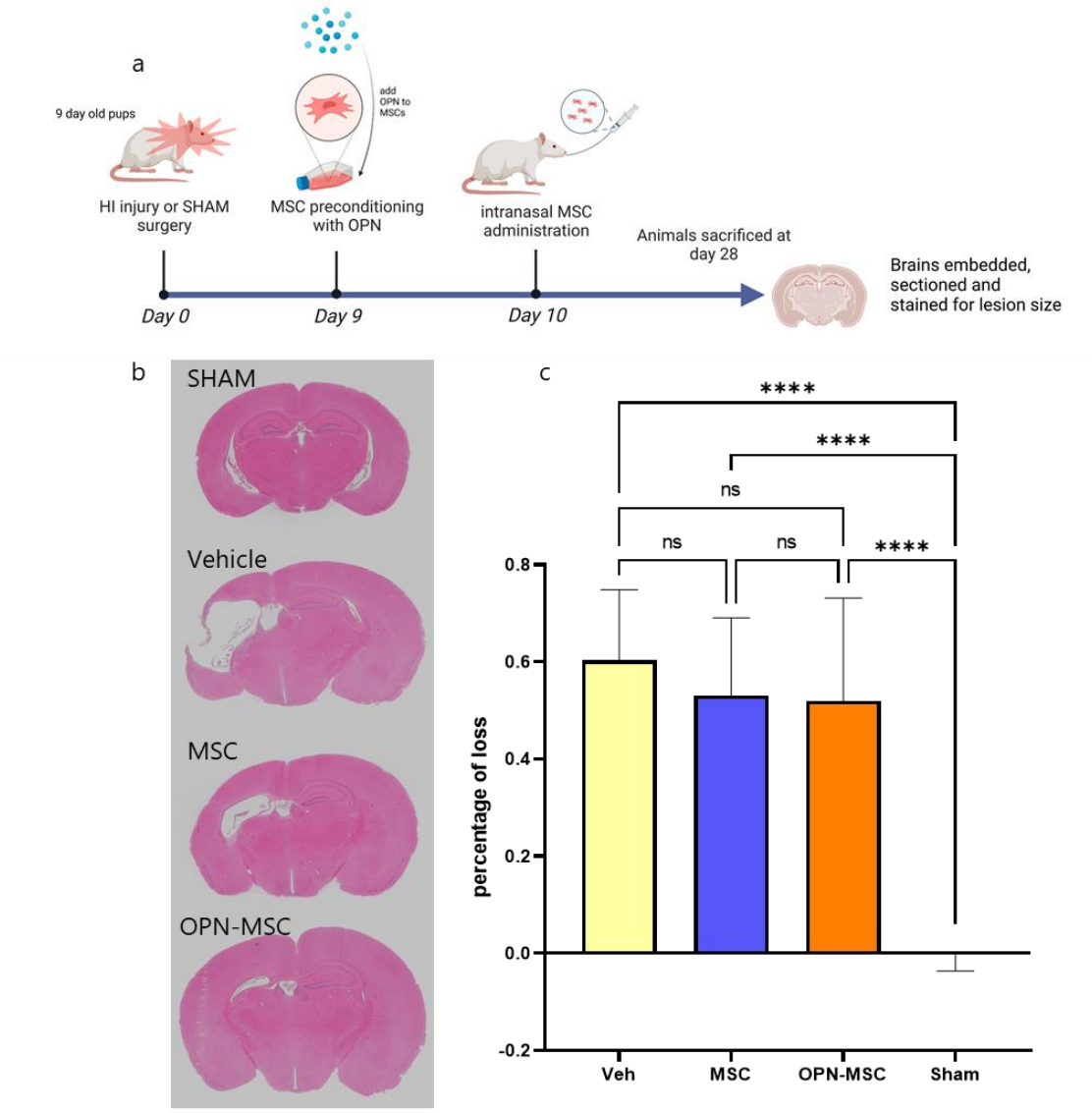

Figure 10 - Intranasal administration of opnMSCs in a neonatal HIE mouse model. *(**a**) Schematic overview of study design. (**b**) Images of H&E stained brain sections from SHAM-operated mice, vehicle treated mice, MSC treated mice and OPN-MSC treated mice. (**c**) Quantification of lesion size by percentage of ipsilateral tissue loss. Data represents mean ±SEM. Statistical analysis (c): one-way ANOVA. **** (P<0.0001). SHAM: n=19, Veh: n=19, MSC: n=18, OPN-MSC: n=19.*

4. Discussion

Neonatal HIE underlies the development of serious neurological and movement disabilities and is one of the leading causes of infant mortality[1,3,6]. Limited treatment options necessitate the development of new innovative treatment methods. Intranasal delivery of MSCs has shown promising results in reducing lesions size and improving motor outcomes in neonatal HIE animal models [26,27,29,36]. The recent translation of this technique into the first clinical application demonstrates its' potential as a future treatment option[37]. Nevertheless, there is room for improvement of treatment efficacy. Optimization strategies for MSC therapy could be detrimental to achieve therapeutic efficacy and applicability for widespread clinical use. It was found that *in vitro* preconditioning of MSCs can improve paracrine potency and therapeutic effects [39]. Extending on this, this research aims to evaluate the potential of OPN preconditioning of MSCs prior to intranasal administration as a strategy to increase the efficacy of intranasal MSC treatment. Additionally, this study aims to elucidate the effect of OPN on the secretome and intracellular pathways of MSCs and thereby gaining insight in the mechanisms responsible for the functional response of OPN preconditioned MSCs.

In this study we showed the secretome of MSCs is changed after preconditioning for 24h with 1000ng/ml OPN. The upregulation of TGF-b mRNA levels in MSCs upon preconditioning is in accordance with another study[64]. While the upregulation of VEGF due to OPN has been shown in other cell types, in this study for the first time it was shown that VEGF mRNA levels are upregulated for MSCs[59]. These genes are involved in many processes concerning the beneficial effects of MSCs. TGF-b secretion by MSCs is associated with anti-apoptotic effects, immunomodulation and tissue repair and VEGF secretion of MSCs associated with anti-apoptotic and angiogenic effects[65–68]. Taken together, the upregulation of these genes suggests an increase in the tissue repair phenotype of OPN-MSCs. The anti-apoptotic, angiogenic and supportive character of the functional effects of VEGF and TGF-b hint at an improved regenerative environment that OPN-MSCs can induce, which can in turn stimulate neuronal precursor cells and enhance differentiation.

The immunomodulatory potential of MSCs is another aspect which seems to be influenced by OPN preconditioning. TGF-b has been shown to be an important factor influencing immune cell activation and functioning, including maturation and activation of microglia [60,69]. TGF-b signalling is important for the prevention of excessive microglia activation. Additionally, silencing TGF-b signalling in mouse models of central nervous system diseases caused uncontrolled microglia reactivity and exacerbation of injury. Other inflammatory genes (iNOS and Cox2) seem to be downregulated and IL-6 seems to be upregulated after OPN preconditioning. These results need to be seen only as hint at downregulation or upregulation, as the results were not significant. However, the sample size for this experiment was rather low (N=3), therefore this experiment should be repeated with a higher sample size. In central nervous system trauma, iNOS and COX2 are both associated with cell death and the pro-inflammatory phase of injury [70,71]. Therefore downregulation of these genes would have to be expected to have beneficial effect regarding modulation of neuroinflammation. However, there seems to be a dual function of these genes. Downregulation of iNOS and COX2 in MSCs have both been reported to have immunostimulatory effects as well as immunosuppressive effects in different settings[70,72–74]. For now it is uncertain whether these genes facilitate a clear pro- or anti-inflammatory downstream effect. Nonetheless, the seemingly down regulation of iNOS and COX2 suggest alterations in the immunomodulatory potential of MSCs due to OPN preconditioning. The apparent upregulation of IL-6 adds to this direction. IL-6 has been indicated as a factor which plays a role in the initiation of inflammation[71]. However, IL-6 is also an important factor of the supportive and anti-inflammatory function of the MSC secretome [60,75]. IL-6,

especially in synergy with TGF-b, has been shown to supress secretion of pro-inflammatory cytokines, induce the synthesis of anti-inflammatory cytokines and induction of regulatory immune cells [76–79]. Finally, there seems to be an upregulation of OPN mRNA levels after OPN preconditioning of MSCs. The modest upregulated OPN mRNA levels indicate that an autocrine positive feedback loop could be activated through OPN binding to its receptors on MSCs. This positive feedback loop mechanism has been suggested in non-small lung cancer cells when OPN interacts with the cell [80]. This indicates that secreted OPN could induce upregulation of OPN secretion from MSCs in that same environment. It was shown that OPN is upregulated in hypoxic preconditioned MSCs (unpublished data). Indicating that a hypoxic area could induce the autocrine positive feedback loop in MSCs, thereby further enhancing OPN production and effect. One limitation of the gene expression experiment in this research is that species have a variation in the mechanisms of MSC mediated immunosuppression[81]. Some anti-inflammatory genes which play an important role in human MSC immunomodulation, are not expressed or very limited expressed in mouse MSCs. For the genes IL-10, IL-13, Il-4, LIF and IL-1a no signal could be detected in this research, while these genes do play a role in human MSC mediated immunosuppression[60]. In future research human MSCs could be used for gene expression analysis for a more clinically relevant characterization of the immunomodulatory potential of OPN-MSCs. Another limitation of the gene expression data is the non-significant data that potentially derive from the low sample size. Therefore, these results need to be looked at with caution and it is advised to repeat these experiments with higher sample sizes.

Several intracellular pathways have been shown to be activated when OPN binds to the cell. The activation of the ERK pathway in general has been implicated as a regulatory factor in many fundamental cellular activities, including migration and proliferation of the cell [82]. The ability of OPN to increase ERK activation through phosphorylation in MSCs has been identified before and similar results were seen in this study [51]. The activation of ERK was suggested to play an important role in the migratory capacity of MSCs. Additionally, another study showed MSCs preconditioned with OPN had a significant increase in their capacity to migrate across a transwell membrane compared to naïve MSCs (unpublished data). Taken together, this indicates the importance of ERK activation for the enhanced migratory capacity of OPN-MSCs. OPNs ability to activate the AKT pathway in MSCs has been shown before and this research showed similar results, however the downstream effects and function are unknown [83]. The AKT pathway is generally involved in the promotion of cell survival and growth [84]. Furthermore, in endothelial cell it was shown that OPN can induce angiogenesis through activation of AKT and ERK, as well as the enhanced expression of VEGF [85]. Taken together, the upregulation of VEGF in MSCs after OPN preconditioning and the activation of both ERK and AKT suggest that a similar function might be operational in OPN-MSCs.

It was shown that the activation of NF-κB is an important factor for the increased immunosuppressive effects of MSCs after TNF-α preconditioning [63,86]. In the current study the activation of NF-κB was indirectly measured by IκB expression. Indeed, IκB is an inhibitor of NF-kB, where IκB sequesters NF-kB in the cytosol[87]. If IκB is reduced or more degraded NF-kB is available to translocate to the nucleus and induce transcription of inflammatory genes. The seemingly small downregulation of IκB, indicating a higher level of available NF- κB in MSCs at the early time point after OPN incubation, poses a promising starting point for further research. However, the small sample size (N=1) requires extreme caution with the interpretation of the results. Thus, the reduction of IκB first needs to be validated with additional experimental samples, before the induction of immunomodulatory response by OPN can be confirmed.

The effect of OPN-MSCs on neurogenesis was analysed in a NSC/MSC co-culture. OPN-MSCs were able to induce differentiation of NSCs into more complex neurons. OPN seems to activate a mechanisms in the MSCs which enhances the secretion of factors which induce the formation of more complex neurons. At this point it is uncertain what these factors are. The aforementioned upregulated genes in OPN-MSCs could be involved, as VEGF and TGF-b have both been associated with neurogenic effects[88,89]. Furthermore it was seen that OPN could induce the differentiation of NSCs into more complex neurons (unpublished data). However many more factors with more prominent effects could be involved, therefore additional research is needed to determine which factors facilitate the increased neurogenic complexity caused by the OPN-MSC secretome.

Additionally, the amount of NSC differentiation towards GFAP+ astrocytes was measured in this study. An increase in the amount $GFAP^+$ area per DAPI stained nucleus was shown, therefore indicating OPN-MSCs seem to enhance the ability of NSCs to differentiate towards astrocytes. Astrocytes play an important role in the central nervous system and are an important factor for recovery after brain injury [90,91]. There are two distinct activation states into which astrocytes can be divided, a neurotoxic state and a neuroprotective state [92,93]. When astrocytes are activated towards a neurotoxic state, they can secrete a variety of pro-inflammatory cytokines. If this state persists for a longer period there is formation of glial scars in the injured areas, which reduces regeneration of the injured tissue [94]. However astrocytes can also be activated towards a neuroprotective phenotype, consisting of more immunosuppressive and supportive characteristics. It has been shown in an adult HIE mouse model that activated astrocytes after MSC treatment were associated with angiogenic properties and functional recovery [90]. In this study an increase in $GFAP^+$ cells was seen in early stages after treatment, without formation of glial scarring in later stages. Therefore, further research is needed to determine whether OPN-MSCs can induce a similar neuroprotective state in astrocytes derived from NSCs. Gene expression, morphology or staining for specific markers could further elucidate what type of reactive state is induced.

Microglia are the most important immune cells in the brain and are the first responders to injury in the central nervous system [95]. The environmental cues determine the activation state of microglia. There are two distinctive states, a toxic pro-inflammatory state that exacerbates neuronal injury and a neuroprotective anti-inflammatory state that promotes recovery and remodelling [96]. The pro-inflammatory state can be activated through LPS incubation, which enhances or maintains the inflammatory state of microglia through secretion of pro-inflammatory cytokines such as TNF-α [97]. In this study, a MSC/microglia co-culture was performed to analyse the immunomodulatory potential of OPN-MSCs. This research showed that microglia were activated by LPS and that MSCs were able to reduce activation as measured by TNF-α, however OPN-MSCs did not further reduce TNF-α secretion compared to naïve MSCs. The ability of MSCs to suppress neuroinflammation is a multifaceted process. Even though the TNF-α secretion of microglia was not lowered further by OPN-MSCs in the co-culture, there could be other mechanisms activated through OPN-MSCs which influence the functional suppression of neuroinflammation. Our results of the gene expression profile indicate that immunomodulatory genes are upregulated in OPN-MSC compared to naïve MSCs. Reduction in other pro-inflammatory cytokines (iNOS, IL-1β, IFN-γ or reactive oxygen species) or an increase in anti-inflammatory factors (IL-10, TGF-b, IGF, or VEGF) secreted by microglia have been linked to a neuroprotective microglia phenotype, these factors could be influenced and need to be assessed in future research[98,99]. Due to the fact that angiogenic and supportive genes are upregulated in OPN-MSCs, there is a higher likelihood that immunomodulatory factors associated with support, repair or immunoregulation, such as CD206 and Arg1, are influenced in microglia [100]. Staining for these particular markers could further elucidate the activation state of microglia upon exposure to the OPN-MSCs secretome.

A limitation of the current microglia/MSC co-culture is that the co-culture set-up is not ideal to mimic the *in vivo* situation during HIE. In the current set-up there is a simultaneous induction of inflammation and addition of the MSCs. This mimics direct inflammation of microglia and the interference of MSCs administered during the initial phase of inflammation. In an *in vivo* setting the MSCs are administered at a later stage. Where, even though there is still an inflammatory environment, the initial stimulus and activator of inflammation has been resolved. Ideally the immunomodulatory potential of OPN-MSCs would be assessed in a *in vivo* model, where brain sections could be stained for markers of microglia activation states. For *in vitro* experiments, the co-culture set-up could be modified. A set-up similar as described by Mukai et al. might be more representative of the *in vivo* situation[101]. Here, microglia are stimulated with LPS for a duration of time, the LPS containing media is removed, microglia are cultured in normal media for a period and only then are the MSCs administered. This allows for the initial stimulus to be removed from the environment, whilst the microglia are still in an inflammatory activated state when the MSCs are administered. Additionally, a more HIE representative manner of microglia activation could be applied to the set-up. Yu et al. describes a cell model where microglia are activated through oxygen–glucose deprivation and reoxygenation to mimic ischemic injury[98].

The overall increased therapeutic efficacy of OPN-MSCs could not be shown after intranasal administration in a neonatal HIE mouse model. There was no difference seen between the vehicle group, MSC group and OPN-MSC group. Multiple previous studies have shown the ability of MSCs to reduce lesion size in a similar neonatal HIE mouse model with the same experimental set-up [27,28,35,37]. A previous study using the same H&E staining as used in the current study showed roughly 30% loss of ipsilateral tissue in the vehicle group and roughly 20% loss of ipsilateral tissue after intranasal MSC administration, respectively (unpublished data). Various other studies showed a reduction in ipsilateral tissue loss from the vehicle group (30-35% loss) to the MSC treated group (15-20% loss) using a MAP2 and MBP staining to quantify the lesion size[27,35,37]. Striking is the considerable lower lesion size of the vehicle group in those studies (30-35% loss) compared the current study (roughly 60 % loss). It is hypothesised that in this study the induction of the HI injury resulted in a too large lesions size for MSCs and OPN-MSCs to activate the endogenous repair mechanisms in this study. The proposed mechanisms of action of intranasally administered MSCs is that they migrate to the lesion area after administration where they secrete factors which activate NSCs in the SVZ and SGZ [19,29,37]. In turn, these NSCs migrate to the lesion where they differentiate into the various neuronal cells and integrate into the tissue. When the lesions size extents through the SVZ and SGZ, there are no NSCs left to facilitate the functional repair MSCs usually induce. It seems that in the performed *in vivo* mouse study a lesion size was induced which destroyed the SVZ and SGZ, thereby eliminating any effect of the MSCs. This hypothesis could be confirmed in further research by staining the brain sections for markers of neuronal precursor cells such as DCX. In order to acquire accurate information about the efficacy of OPN-MSC compared to naïve MSCs the mouse study should be repeated with a similar experimental set-up, where ideally the induced lesion size would be reduced.

The overall increased therapeutic efficacy of OPN-MSCs could not be shown after intranasal administration in a neonatal HIE mouse model. There was no difference seen between the vehicle group, MSC group and OPN-MSC group. Multiple previous studies have shown the ability of MSCs to reduce lesion size in a similar neonatal HIE mouse model with the same experimental set-up [27,28,36,38]. A previous study using the same H&E staining used in this research showed a lesion size reduction from the vehicle group with roughly 30% loss of ipsilateral tissue to a loss of roughly 20% of ipsilateral tissue after intranasal MSC administration (unpublished data). Various other studies

showed a reduction in ipsilateral tissue loss from the vehicle group (30-35% loss) to the MSC treated group (15-20% loss) using a MAP2 and MBP staining to quantify the lesion size[27,36,38]. What is striking is the considerable lower lesion size of the vehicle group in those studies (30-35% loss) compared to the lesion size of the vehicle group of the mouse study performed in this research (roughly 60 % loss). It is hypothesised that in this study the induction of the HI injury resulted in a too large lesions size for MSCs and OPN-MSCs to activate the endogenous repair mechanisms in this study. The proposed mechanisms of action of intranasally administered MSCs is that they migrate to the lesion area after administration where they secrete factors which activate NSCs in the SVZ and SGZ [19,29,38]. In turn, these NSCs migrate to the lesion where they differentiate into the various neuronal cell lines and integrate into the tissue. When the lesions size extents through the SVZ and SGZ, there are no NSCs left which can facilitate the functional repair MSCs usually induce. It seems that in the performed *in vivo* mouse study a lesion size was induced which destroyed the SVZ and SGZ, thereby eliminating any effect of the MSCs. This hypothesis could be confirmed in further research by staining the brain sections for markers of neuronal precursor cells such as DCX. In order to acquire accurate information about the efficacy of OPN-MSC compared to naïve MSCs the mouse study should be repeated with a similar experimental set-up, where ideally the induced lesion size would be reduced.

Together, the findings of this study suggest that OPN preconditioning of MSCs activates various intracellular pathways and modulates the paracrine potency of the cells. The angiogenic and growth supportive capacities of OPN-MSCs compared to naïve MSCs seem to be upregulated. Additionally, although the OPN-MSC secretome did not alter microglial responses to LPS, intracellular pathways and gene expression associated with inflammation in MSCs seem to be affected after OPN preconditioning. Consequently, the secretome of OPN-MSCs may be altered in terms of immunomodulatory potential. How the seemingly altered immunomodulatory capacity of OPN-MSCs translates into functional effects is still unclear, further research is needed to better understand the effects on neuroinflammation and immunomodulation. The secretome of OPN-MSCs also increased differentiation of NSCs towards astrocytes and induced NSCs into the formation of more complex neurons. The overall therapeutic efficacy needs to be elucidated in another in vivo mouse study. The changes in the secretome and the increased neurogenic capacity of the OPN-MSCs indicate that there is a potential for therapeutical benefits compared to naïve MSCs for neonatal HIE injury.

5. References

1. Russ JB, Simmons R, Glass HC. Neonatal encephalopathy: Beyond hypoxic-ischemic encephalopathy. *Neoreviews*. 2021;22(3):e148-e162. doi:10.1542/neo.22-3-e148

2. Reid SM, Meehan E, Mcintyre S, Goldsmith S, Badawi N, Reddihough DS. Temporal trends in cerebral palsy by impairment severity and birth gestation. *Dev Med Child Neurol*. 2016;58:25-35. doi:10.1111/DMCN.13001

3. Thornberg E, Thiringer K, Odeback A, Milsom I. Birth asphyxia: incidence, clinical course and outcome in a Swedish population. *Acta Pædiatrica*. 1995;84(8):927-932. doi:10.1111/J.1651-2227.1995.TB13794.X

4. Lee ACC, Kozuki N, Blencowe H, et al. Intrapartum-related neonatal encephalopathy incidence and impairment at regional and global levels for 2010 with trends from 1990. *Pediatr Res 2013 741*. 2013;74(1):50-72. doi:10.1038/PR.2013.206

5. Glass HC, Shellhaas RA, Wusthoff CJ, et al. Contemporary Profile of Seizures in Neonates: A Prospective Cohort Study. *J Pediatr*. 2016;174:98-103.e1. doi:10.1016/J.JPEDS.2016.03.035

6. Lawn J, Shibuya K, Stein C. No cry at birth: global estimates of intrapartum stillbirths and intrapartum-related neonatal deaths. *Bull World Health Organ*. 2005;83(6):409. doi:/S0042-96862005000600008

7. Lawn JE, Lee ACC, Kinney M, et al. Two million intrapartum-related stillbirths and neonatal deaths: Where, why, and what can be done? *Int J Gynecol Obstet*. 2009;107(Supplement):S5-S19. doi:10.1016/J.IJGO.2009.07.016

8. Murray CJL, Lopez AD. Global mortality, disability, and the contribution of risk factors: Global burden of disease study. *Lancet*. 1997;349(9063):1436-1442. doi:10.1016/S0140-6736(96)07495-8

9. Douglas-Escobar M, Weiss MD. Hypoxic-Ischemic Encephalopathy AReview for the Clinician. 2015;169(4):397-403. doi:10.1001/JAMAPEDIATRICS.2014.3269

10. Worden LT, Massey SL. Therapeutic Hypothermia Effects on Brain Development. *Pract Neurol*. 2020;(March/April):31-46. https://practicalneurology.com/articles/2020-mar-apr/therapeutic-hypothermia-effects-on-brain-development/pdf

11. Gunn AJ, Thoresen M. Neonatal encephalopathy and hypoxic–ischemic encephalopathy. *Handb Clin Neurol*. 2019;162:217-237. doi:10.1016/B978-0-444-64029-1.00010-2

12. Johnston M V., Fatemi A, Wilson MA, Northington F. Treatment advances in neonatal neuroprotection and neurointensive care. *Lancet Neurol*. 2011;10(4):372-382. doi:10.1016/S1474-4422(11)70016-3

13. Davidson JO, Gonzalez F, Gressens P, Gunn AJ. Update on mechanisms of the pathophysiology of neonatal encephalopathy. *Semin Fetal Neonatal Med*. 2021;26(5):101267. doi:10.1016/J.SINY.2021.101267

14. Azzopard D, Wyatt JS, Cady EB, et al. Prognosis of Newborn Infants with Hypoxic-Ischemic Brain Injury Assessed by Phosphorus Magnetic Resonance Spectroscopy. *Pediatr Res 1989 255*. 1989;25(5):445-451. doi:10.1203/00006450-198905000-00004

15. Fleiss B, Gressens P. Tertiary mechanisms of brain damage: a new hope for treatment of cerebral palsy? *Lancet Neurol*. 2012;11(6):556-566. doi:10.1016/S1474-4422(12)70058-3

16. Tagin MA, Woolcott CG, Vincer MJ, Whyte RK, Stinson DA. Hypothermia for Neonatal Hypoxic

Ischemic Encephalopathy: An Updated Systematic Review and Meta-analysis. *Arch Pediatr Adolesc Med*. 2012;166(6):558-566. doi:10.1001/ARCHPEDIATRICS.2011.1772

17. Shankaran S, Natarajan G, Chalak L, Pappas A, McDonald SA, Laptook AR. HYPOTHERMIA for NEONATAL HYPOXIC-ISCHEMIC ENCEPHALOPATHY: NICHD NEONATAL RESEARCH NETWORK CONTRIBUTION to the FIELD. *Semin Perinatol*. 2016;40(6):385. doi:10.1053/J.SEMPERI.2016.05.009

18. Yang Z, Covey M V., Bitel CL, Ni L, Jonakait GM, Levison SW. Sustained neocortical neurogenesis after neonatal hypoxic/ischemic injury. *Ann Neurol*. 2007;61(3):199-208. doi:10.1002/ANA.21068

19. Qu R, Li Y, Gao Q, et al. Neurotrophic and growth factor gene expression profiling of mouse bone marrow stromal cells induced by ischemic brain extracts. *Neuropathology*. 2007;27(4):355. doi:10.1111/J.1440-1789.2007.00792.X

20. Fleiss B, Guillot P V., Titomanlio L, Baud O, Hagberg H, Gressens P. Stem Cell Therapy for Neonatal Brain Injury. *Clin Perinatol*. 2014;41(1):133-148. doi:10.1016/J.CLP.2013.09.002

21. Manochantr S, U-pratya Y, Kheolamai P, et al. Immunosuppressive properties of mesenchymal stromal cells derived from amnion, placenta, Wharton's jelly and umbilical cord. *Intern Med J*. 2013;43(4):430-439. doi:10.1111/IMJ.12044

22. Chen Y, Shao JZ, Xiang LX, Dong XJ, Zhang GR. Mesenchymal stem cells: A promising candidate in regenerative medicine. *Int J Biochem Cell Biol*. 2008;40(5):815-820. doi:10.1016/J.BIOCEL.2008.01.007

23. Yoo SW, Kim SS, Lee SY, et al. Mesenchymal stem cells promote proliferation of endogenous neural stem cells and survival of newborn cells in a rat stroke model. *Exp Mol Med 2008 404*. 2008;40(4):387-397. doi:10.3858/emm.2008.40.4.387

24. Chen J, Li Y, Katakowski M, et al. Intravenous bone marrow stromal cell therapy reduces apoptosis and promotes endogenous cell proliferation after stroke in female rat. *J Neurosci Res*. 2003;73(6):778-786. doi:10.1002/JNR.10691

25. Kang SK, Shin IS, Ko MS, Jo JY, Ra JC. Journey of mesenchymal stem cells for homing: Strategies to enhance efficacy and safety of stem cell therapy. *Stem Cells Int*. Published online 2012. doi:10.1155/2012/342968

26. van Velthoven CTJ, Kavelaars A, van Bel F, Heijnen CJ. Mesenchymal stem cell treatment after neonatal hypoxic-ischemic brain injury improves behavioral outcome and induces neuronal and oligodendrocyte regeneration. *Brain Behav Immun*. 2010;24(3):387-393. doi:10.1016/J.BBI.2009.10.017

27. Donega V, van Velthoven CTJ, Nijboer CH, et al. Intranasal Mesenchymal Stem Cell Treatment for Neonatal Brain Damage: Long-Term Cognitive and Sensorimotor Improvement. *PLoS One*. 2013;8(1). doi:10.1371/JOURNAL.PONE.0051253

28. Lee JA, Kim B Il, Jo CH, et al. Mesenchymal Stem-Cell Transplantation for Hypoxic-Ischemic Brain Injury in Neonatal Rat Model. *Pediatr Res 2010 671*. 2010;67(1):42-46. doi:10.1203/pdr.0b013e3181bf594b

29. Van Velthoven CTJ, Kavelaars A, Van Bel F, Heijnen CJ. Mesenchymal stem cell transplantation changes the gene expression profile of the neonatal ischemic brain. *Brain Behav Immun*. 2011;25(7):1342-1348. doi:10.1016/J.BBI.2011.03.021

30. Fischer UM, Harting MT, Jimenez F, et al. Pulmonary Passage is a Major Obstacle for

Intravenous Stem Cell Delivery: The Pulmonary First-Pass Effect. *Stem Cells Dev*. 2009;18(5):683. doi:10.1089/SCD.2008.0253

31. Marquez-Curtis LA, Janowska-Wieczorek A. Enhancing the migration ability of mesenchymal stromal cells by targeting the SDF-1/CXCR4 axis. *Biomed Res Int*. 2013;2013. doi:10.1155/2013/561098

32. Eggenhofer E, Benseler V, Kroemer A, et al. Mesenchymal stem cells are short-lived and do not migrate beyond the lungs after intravenous infusion. *Front Immunol*. 2012;3(SEP). doi:10.3389/FIMMU.2012.00297

33. Wagenaar N, Nijboer CH, van Bel F. Repair of neonatal brain injury: bringing stem cell-based therapy into clinical practice. *Dev Med Child Neurol*. 2017;59(10):997-1003. doi:10.1111/DMCN.13528/ABSTRACT

34. Van Velthoven CTJ, Kavelaars A, Van Bel F, Heijnen CJ. Repeated mesenchymal stem cell treatment after neonatal hypoxia-ischemia has distinct effects on formation and maturation of new neurons and oligodendrocytes leading to restoration of damage, corticospinal motor tract activity, and sensorimotor function. *J Neurosci*. 2010;30(28):9603-9611. doi:10.1523/JNEUROSCI.1835-10.2010

35. Chapman CD, Frey WH, Craft S, et al. Intranasal Treatment of Central Nervous System Dysfunction in Humans. *Pharm Res*. 2013;30(10):2475. doi:10.1007/S11095-012-0915-1

36. Donega V, Nijboer CH, Van Velthoven CTJ, et al. Assessment of long-term safety and efficacy of intranasal mesenchymal stem cell treatment for neonatal brain injury in the mouse. *Pediatr Res 2015 785*. 2015;78(5):520-526. doi:10.1038/pr.2015.145

37. Baak LM, Wagenaar N, van der Aa NE, et al. Feasibility and safety of intranasally administered mesenchymal stromal cells after perinatal arterial ischaemic stroke in the Netherlands (PASSIoN): a first-in-human, open-label intervention study. *Lancet Neurol*. 2022;21(6):528-536. doi:10.1016/S1474-4422(22)00117-X

38. Donega V, Nijboer CH, van Tilborg G, Dijkhuizen RM, Kavelaars A, Heijnen CJ. Intranasally administered mesenchymal stem cells promote a regenerative niche for repair of neonatal ischemic brain injury. *Exp Neurol*. 2014;261:53-64. doi:10.1016/J.EXPNEUROL.2014.06.009

39. Park WS, Ahn SY, Sung SI, Ahn JY, Chang YS. Strategies to enhance paracrine potency of transplanted mesenchymal stem cells in intractable neonatal disorders. *Pediatr Res 2018 831*. 2017;83(1):214-222. doi:10.1038/pr.2017.249

40. Doorn J, Moll G, Le Blanc K, Van Blitterswijk C, De Boer J. Therapeutic applications of mesenchymal stromal cells: paracrine effects and potential improvements. *Tissue Eng Part B Rev*. 2012;18(2):101-115. doi:10.1089/TEN.TEB.2011.0488

41. Waszak P, Alphonse R, Vadivel A, Ionescu L, Eaton F, Thébaud B. Preconditioning enhances the paracrine effect of mesenchymal stem cells in preventing oxygen-induced neonatal lung injury in rats. *Stem Cells Dev*. 2012;21(15):2789-2797. doi:10.1089/SCD.2010.0566

42. Rota C, Imberti B, Pozzobon M, et al. Human amniotic fluid stem cell preconditioning improves their regenerative potential. *Stem Cells Dev*. 2012;21(11):1911-1923. doi:10.1089/SCD.2011.0333

43. Heo SC, Jeon ES, Lee IH, Kim HS, Kim MB, Kim JH. Tumor necrosis factor-α-activated human adipose tissue-derived mesenchymal stem cells accelerate cutaneous wound healing through paracrine mechanisms. *J Invest Dermatol*. 2011;131(7):1559-1567. doi:10.1038/JID.2011.64

44. Tang Y, Cai B, Yuan F, et al. Melatonin Pretreatment Improves the Survival and Function of Transplanted Mesenchymal Stem Cells after Focal Cerebral Ischemia. *Cell Transplant*. 2014;23(10):1279-1291. doi:10.3727/096368913X667510

45. Yao Y, Zhang F, Wang L, et al. Lipopolysaccharide preconditioning enhances the efficacy of mesenchymal stem cells transplantation in a rat model of acute myocardial infarction. *J Biomed Sci*. 2009;16(1). doi:10.1186/1423-0127-16-74

46. Najafi R, Sharifi AM. Deferoxamine preconditioning potentiates mesenchymal stem cell homing in vitro and in streptozotocin-diabetic rats. *Expert Opin Biol Ther*. 2013;13(7):959-972. doi:10.1517/14712598.2013.782390

47. Cui X, Wang H, Guo H, et al. Transplantation of mesenchymal stem cells preconditioned with diazoxide, a mitochondrial ATP-sensitive potassium channel opener, promotes repair of myocardial infarction in rats. *Tohoku J Exp Med*. 2010;220(2):139-147. doi:10.1620/TJEM.220.139

48. Kahles F, Findeisen HM, Bruemmer D. Osteopontin: A novel regulator at the cross roads of inflammation, obesity and diabetes. *Mol Metab*. 2014;3(4):384-393. doi:10.1016/J.MOLMET.2014.03.004

49. Rangaswami H, Bulbule A, Kundu GC. Osteopontin: role in cell signaling and cancer progression. *Trends Cell Biol*. 2006;16(2):79-87. doi:10.1016/J.TCB.2005.12.005

50. Wang KX, Denhardt DT. Osteopontin: role in immune regulation and stress responses. *Cytokine Growth Factor Rev*. 2008;19(5-6):333-345. doi:10.1016/J.CYTOGFR.2008.08.001

51. Zou C, Luo Q, Qin J, et al. Osteopontin Promotes Mesenchymal Stem Cell Migration and Lessens Cell Stiffness via Integrin β1, FAK, and ERK Pathways. *Cell Biochem Biophys*. 2013;65(3):455-462. doi:10.1007/S12013-012-9449-8/FIGURES/4

52. Rabenstein M, Hucklenbroich J, Willuweit A, et al. Osteopontin mediates survival, proliferation and migration of neural stem cells through the chemokine receptor CXCR4. *Stem Cell Res Ther*. 2015;6(1). doi:10.1186/S13287-015-0098-X

53. Kalluri HSG, Dempsey RJ. Osteopontin increases the proliferation of neural progenitor cells. *Int J Dev Neurosci*. 2012;30(5):359-362. doi:10.1016/J.IJDEVNEU.2012.04.003

54. Yan YP, Lang BT, Vemuganti R, Dempsey RJ. Osteopontin is a mediator of the lateral migration of neuroblasts from the subventricular zone after focal cerebral ischemia. *Neurochem Int*. 2009;55(8):826-832. doi:10.1016/J.NEUINT.2009.08.007

55. Van Velthoven CTJ, Heijnen CJ, Van Bel F, Kavelaars A. Osteopontin enhances endogenous repair after neonatal hypoxic-ischemic brain injury. *Stroke*. 2011;42(8):2294-2301. doi:10.1161/STROKEAHA.110.608315

56. Marcondes MCG, Poling M, Watry DD, Hall DS, Fox HS. In vivo osteopontin-induced macrophage accumulation is dependent on CD44 expression. *Cell Immunol*. 2008;254(1):56-62. doi:10.1016/J.CELLIMM.2008.06.012

57. Uede T. Osteopontin, intrinsic tissue regulator of intractable inflammatory diseases. *Pathol Int*. 2011;61(5):265-280. doi:10.1111/J.1440-1827.2011.02649.X

58. Gong L, Manaenko A, Fan R, et al. Osteopontin attenuates inflammation via JAK2/STAT1 pathway in hyperglycemic rats after intracerebral hemorrhage. *Neuropharmacology*. 2018;138:160. doi:10.1016/J.NEUROPHARM.2018.06.009

59. Carvalho MS, Cabral JMS, da Silva CL, Vashishth D. Synergistic effect of extracellularly

supplemented osteopontin and osteocalcin on stem cell proliferation, osteogenic differentiation, and angiogenic properties. *J Cell Biochem*. 2019;120(4):6555-6569. doi:10.1002/JCB.27948

60. D K, I B, E I-T, et al. Secretion of immunoregulatory cytokines by mesenchymal stem cells. *World J Stem Cells*. 2014;6(5):552. doi:10.4252/WJSC.V6.I5.552

61. Meloche S, Pouysségur J. The ERK1/2 mitogen-activated protein kinase pathway as a master regulator of the G1- to S-phase transition. *Oncogene*. 2007;26(22):3227-3239. doi:10.1038/SJ.ONC.1210414

62. Manning BD, Cantley LC. AKT/PKB signaling: navigating downstream. *Cell*. 2007;129(7):1261-1274. doi:10.1016/J.CELL.2007.06.009

63. Dorronsoro A, Ferrin I, Salcedo JM, et al. Human mesenchymal stromal cells modulate T-cell responses through TNF-α-mediated activation of NF-κB. *Eur J Immunol*. 2014;44(2):480-488. doi:10.1002/EJI.201343668

64. Weber CE, Kothari AN, Wai PY, et al. Osteopontin mediates an MZF1-TGF-β1-dependent transformation of mesenchymal stem cells into cancer-associated fibroblasts in breast cancer. *Oncogene*. 2015;34(37):4821-4833. doi:10.1038/ONC.2014.410

65. Lichtman MK, Otero-Vinas M, Falanga V. Transforming growth factor beta (TGF-β) isoforms in wound healing and fibrosis. *Wound Repair Regen*. 2016;24(2):215-222. doi:10.1111/WRR.12398

66. Rehman J, Traktuev D, Li J, et al. Secretion of angiogenic and antiapoptotic factors by human adipose stromal cells. *Circulation*. 2004;109(10):1292-1298. doi:10.1161/01.CIR.0000121425.42966.F1

67. Nicola M Di, Carlo-Stella C, Magni M, et al. Human bone marrow stromal cells suppress T-lymphocyte proliferation induced by cellular or nonspecific mitogenic stimuli. *Blood*. 2002;99(10):3838-3843. doi:10.1182/BLOOD.V99.10.3838

68. Kinnaird T, Stabile E, Burnett MS, et al. Local delivery of marrow-derived stromal cells augments collateral perfusion through paracrine mechanisms. *Circulation*. 2004;109(12):1543-1549. doi:10.1161/01.CIR.0000124062.31102.57

69. Spittau B, Dokalis N, Prinz M. The Role of TGFβ Signaling in Microglia Maturation and Activation. *Trends Immunol*. 2020;41(9):836-848. doi:10.1016/J.IT.2020.07.003

70. Hu X, Nesic-Taylor O, Qiu J, et al. Activation of nuclear factor-kappaB signaling pathway by interleukin-1 after hypoxia/ischemia in neonatal rat hippocampus and cortex. *J Neurochem*. 2005;93(1):26-37. doi:10.1111/J.1471-4159.2004.02968.X

71. Hagberg H, Mallard C, Ferriero DM, et al. The role of inflammation in perinatal brain injury. *Nat Rev Neurol 2015 114*. 2015;11(4):192-208. doi:10.1038/nrneurol.2015.13

72. Han Y, Yang J, Fang J, et al. The secretion profile of mesenchymal stem cells and potential applications in treating human diseases. *Signal Transduct Target Ther*. 2022;7(1). doi:10.1038/S41392-022-00932-0

73. Li W, Ren G, Huang Y, et al. Mesenchymal stem cells: a double-edged sword in regulating immune responses. *Cell Death Differ*. 2012;19(9):1505-1513. doi:10.1038/CDD.2012.26

74. Poligone B, Baldwin AS. Positive and negative regulation of NF-kappaB by COX-2: roles of different prostaglandins. *J Biol Chem*. 2001;276(42):38658-38664. doi:10.1074/JBC.M106599200

75. da Silva Meirelles L, Fontes AM, Covas DT, Caplan AI. Mechanisms involved in the therapeutic properties of mesenchymal stem cells. *Cytokine Growth Factor Rev*. 2009;20(5-6):419-427. doi:10.1016/J.CYTOGFR.2009.10.002

76. Xing Z, Gauldie J, Cox G, et al. IL-6 is an antiinflammatory cytokine required for controlling local or systemic acute inflammatory responses. *J Clin Invest*. 1998;101(2):311-320. doi:10.1172/JCI1368

77. Tilg H, Trehu E, Atkins MB, Dinarello CA, Mier JW. Interleukin-6 (IL-6) as an Anti-inflammatory Cytokine: Induction of Circulating IL-1 Receptor Antagonist and Soluble Tumor Necrosis Factor Receptor p55. *Blood*. 1994;83(1):113-118. doi:10.1182/BLOOD.V83.1.113.113

78. Steensberg A, Fischer CP, Keller C, Møller K, Pedersen BK. IL-6 enhances plasma IL-1ra, IL-10, and cortisol in humans. *Am J Physiol Endocrinol Metab*. 2003;285(2). doi:10.1152/AJPENDO.00074.2003

79. Nakagawa T, Tsuruoka M, Ogura H, et al. IL-6 positively regulates Foxp3+CD8+ T cells in vivo. *Int Immunol*. 2010;22(2):129-139. doi:10.1093/INTIMM/DXP119

80. Choi SI, Kim SY, Lee JH, Kim JY, Cho EW, Kim IG. Osteopontin production by TM4SF4 signaling drives a positive feedback autocrine loop with the STAT3 pathway to maintain cancer stem cell-like properties in lung cancer cells. *Oncotarget*. 2017;8(60):101284-101297. doi:10.18632/ONCOTARGET.21021

81. Ren G, Su J, Zhang L, et al. Species variation in the mechanisms of mesenchymal stem cell-mediated immunosuppression. *Stem Cells*. 2009;27(8):1954-1962. doi:10.1002/STEM.118

82. Howe AK, Aplin AE, Juliano RL. Anchorage-dependent ERK signaling - Mechanisms and consequences. *Curr Opin Genet Dev*. 2002;12(1):30-35. doi:10.1016/S0959-437X(01)00260-X

83. Lee MN, Song JH, Oh SH, et al. The primary cilium directs osteopontin-induced migration of mesenchymal stem cells by regulating CD44 signaling and Cdc42 activation. *Stem Cell Res*. 2020;45. doi:10.1016/J.SCR.2020.101799

84. Nitulescu GM, Van De Venter M, Nitulescu G, et al. The Akt pathway in oncology therapy and beyond (Review). *Int J Oncol*. 2018;53(6):2319-2331. doi:10.3892/IJO.2018.4597

85. Dai J, Peng L, Fan K, et al. Osteopontin induces angiogenesis through activation of PI3K/AKT and ERK1/2 in endothelial cells. *Oncogene 2009 2838*. 2009;28(38):3412-3422. doi:10.1038/onc.2009.189

86. Li H, Dai H, Li J. Immunomodulatory properties of mesenchymal stromal/stem cells: The link with metabolism. *J Adv Res*. 2023;45:15-29. doi:10.1016/J.JARE.2022.05.012

87. Mulero MC, Huxford T, Ghosh G. NF-κB, IκB, and IKK: Integral Components of Immune System Signaling. *Adv Exp Med Biol*. 2019;1172:207-226. doi:10.1007/978-981-13-9367-9_10

88. Carmeliet P, Storkebaum E. Vascular and neuronal effects of VEGF in the nervous system: implications for neurological disorders. *Semin Cell Dev Biol*. 2002;13(1):39-53. doi:10.1006/SCDB.2001.0290

89. Meyers EA, Kessler JA. TGF-β Family Signaling in Neural and Neuronal Differentiation, Development, and Function. *Cold Spring Harb Perspect Biol*. 2017;9(8). doi:10.1101/CSHPERSPECT.A022244

90. Cho SR, Suh H, Yu JH, Kim HH, Seo JH, Seo CH. Astroglial Activation by an Enriched Environment after Transplantation of Mesenchymal Stem Cells Enhances Angiogenesis after Hypoxic-Ischemic Brain Injury. *Int J Mol Sci*. 2016;17(9). doi:10.3390/IJMS17091550

91. Li Y, Liu Z, Xin H, Chopp M. The role of astrocytes in mediating exogenous cell-based restorative therapy for stroke. *Glia*. 2014;62(1):1-16. doi:10.1002/GLIA.22585

92. Zamanian JL, Xu L, Foo LC, et al. Genomic analysis of reactive astrogliosis. *J Neurosci*. 2012;32(18):6391-6410. doi:10.1523/JNEUROSCI.6221-11.2012

93. Liddelow SA, Barres BA. Reactive Astrocytes: Production, Function, and Therapeutic Potential. *Immunity*. 2017;46(6):957-967. doi:10.1016/J.IMMUNI.2017.06.006

94. Wanner IB, Anderson MA, Song B, et al. Glial scar borders are formed by newly proliferated, elongated astrocytes that interact to corral inflammatory and fibrotic cells via STAT3-dependent mechanisms after spinal cord injury. *J Neurosci*. 2013;33(31):12870-12886. doi:10.1523/JNEUROSCI.2121-13.2013

95. Saijo K, Glass CK. Microglial cell origin and phenotypes in health and disease. *Nat Rev Immunol*. 2011;11(11):775-787. doi:10.1038/NRI3086

96. Hu X, Leak RK, Shi Y, et al. Microglial and macrophage polarization—new prospects for brain repair. *Nat Rev Neurol*. 2015;11(1):56-64. doi:10.1038/NRNEUROL.2014.207

97. Askari VR, Shafiee-Nick R. The protective effects of β-caryophyllene on LPS-induced primary microglia M1/M2 imbalance: A mechanistic evaluation. *Life Sci*. 2019;219:40-73. doi:10.1016/J.LFS.2018.12.059

98. Yu H, Xu Z, Qu G, et al. Hypoxic Preconditioning Enhances the Efficacy of Mesenchymal Stem Cells-Derived Conditioned Medium in Switching Microglia toward Anti-inflammatory Polarization in Ischemia/Reperfusion. *Cell Mol Neurobiol*. 2021;41(3):505-524. doi:10.1007/S10571-020-00868-5

99. Lan X, Han X, Li Q, Yang QW, Wang J. Modulators of microglial activation and polarization after intracerebral haemorrhage. *Nat Rev Neurol*. 2017;13(7):420-433. doi:10.1038/NRNEUROL.2017.69

100. Chhor V, Le Charpentier T, Lebon S, et al. Characterization of phenotype markers and neuronotoxic potential of polarised primary microglia in vitro. *Brain Behav Immun*. 2013;32:70-85. doi:10.1016/J.BBI.2013.02.005

101. Mukai T, Di Martino E, Tsuji S, Blomgren K, Nagamura-Inoue T, Ådén U. Umbilical cord-derived mesenchymal stromal cells immunomodulate and restore actin dynamics and phagocytosis of LPS-activated microglia via PI3K/Akt/Rho GTPase pathway. *Cell Death Discov 2021 71*. 2021;7(1):1-13. doi:10.1038/s41420-021-00436-w

Appendix

A. qPCR

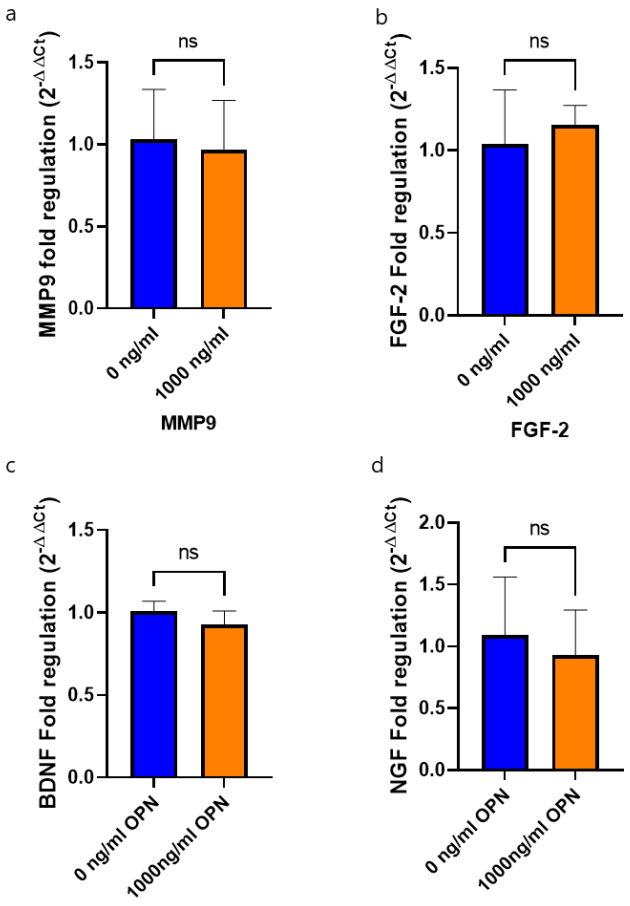

Figure 11 - Gene expression of naïve MSCs compared to MSCs preconditioned with 1000 ng/ml OPN for 24 hours determined by qPCR. *(**a-d**) Fold regulation of MMP9, FGF-2, BDNF and NGF mRNA normalized to naïve MSC. Data represents mean ± SEM. Statistical analysis (a-g): unpaired t-test. *(p<0.05). (a-d): n=3*

B. Western blot

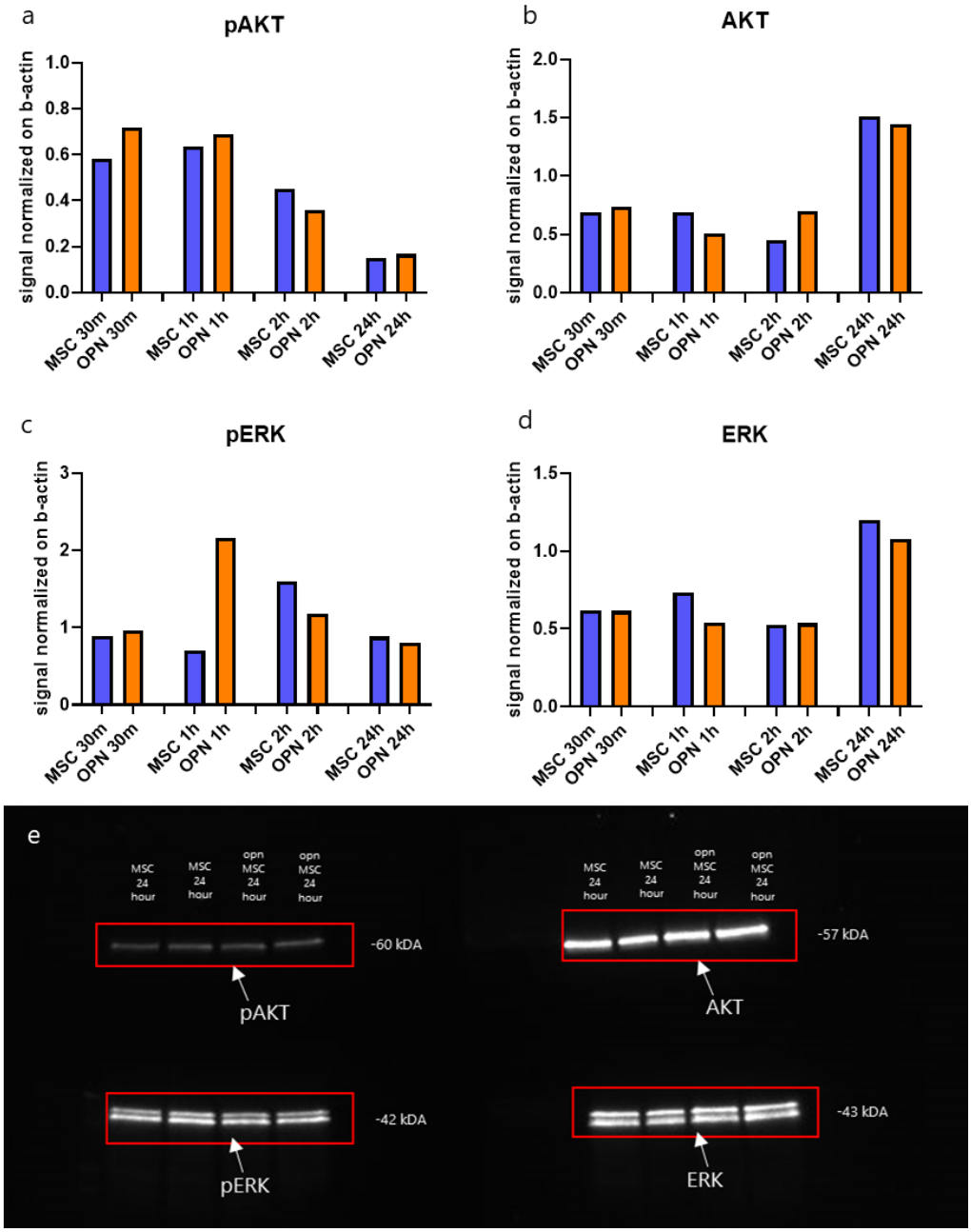

Figure 12 - ***Western blot analysis of (p)ERK, (p)AKT expression of MSCs after OPN incubation at different time points.*** *(**a**) Expression of pAKT in MSCs measured after 30 minutes, 1 hour, 2hours and 24 hours of incubation with OPN compared to naïve MSCs. (**b**) Expression of AKT in MSCs measured after 30 minutes, 1 hour, 2hours and 24 hours of incubation with OPN compared to naïve MSCs. (**c**) Expression of pERK in MSCs measured after 30 minutes, 1 hour, 2hours and 24 hours of incubation with OPN compared to naïve MSCs. (**d**) Expression of ERK in MSCs measured after 30 minutes, 1 hour, 2hours and 24 hours of incubation with OPN compared to naïve MSCs. (**e**) Western blot image of (p)AKT and (p)ERK expression in MSCs after 24 hours of incubation with OPN compared to naïve MSCs. Data represents mean (a-e): MSC n=1, OPN-MSC n=1.*

C. MSC/NSC co-culture

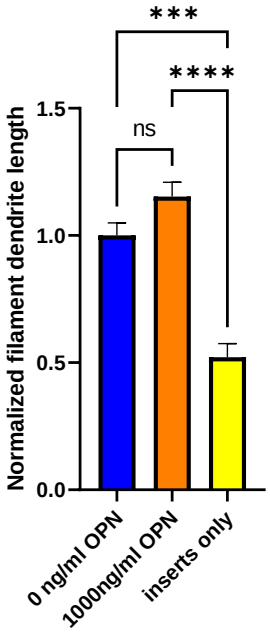

Figure 13 - ***Morphological analysis of non-contact MSC/NSC co-culture.*** *Average filament dendrite length normalized to naïve MSCs (0 ng/ml). Data represents mean ± SD. Statistical analysis (c-e, g): one-way ANOVA. ***(p<0.001), ***(p<0.0001). (c-d, g): 0 ng/ml: n=12, 1000 ng/ml : n=10, inserts only: n=5.*